



**HAL**  
open science

# The Get1/2 insertase forms a channel to mediate the insertion of tail-anchored proteins into the ER

Paul Heo, Jacob A Culver, Jennifer Miao, Frederic Pincet, Malaiyalam Mariappan

► **To cite this version:**

Paul Heo, Jacob A Culver, Jennifer Miao, Frederic Pincet, Malaiyalam Mariappan. The Get1/2 insertase forms a channel to mediate the insertion of tail-anchored proteins into the ER. Cell Reports, 2023, 42 (1), pp.111921. 10.1016/j.celrep.2022.111921 . hal-04116419

**HAL Id: hal-04116419**

**<https://u-paris.hal.science/hal-04116419v1>**

Submitted on 4 Jun 2023

**HAL** is a multi-disciplinary open access archive for the deposit and dissemination of scientific research documents, whether they are published or not. The documents may come from teaching and research institutions in France or abroad, or from public or private research centers.

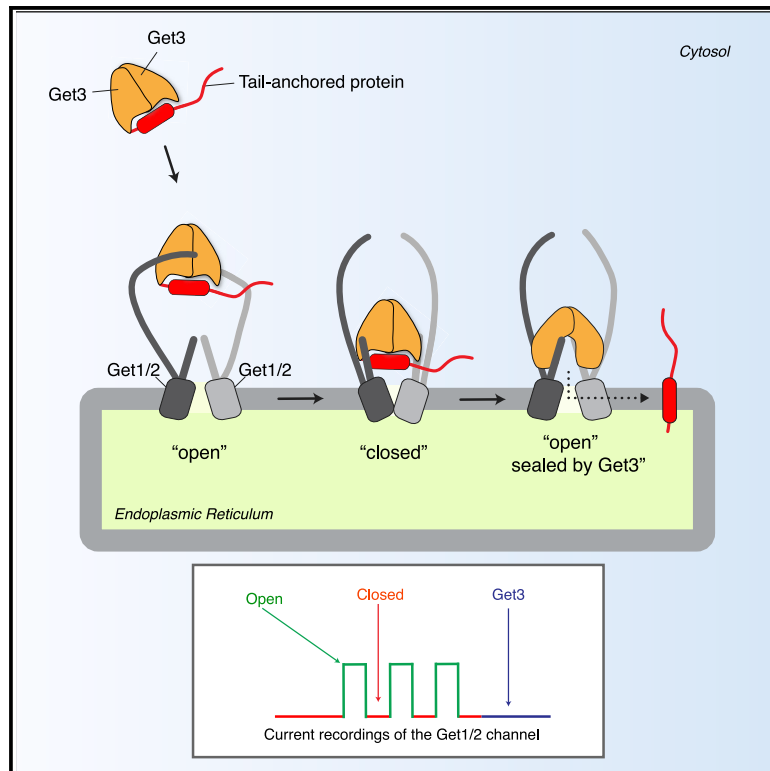
L'archive ouverte pluridisciplinaire **HAL**, est destinée au dépôt et à la diffusion de documents scientifiques de niveau recherche, publiés ou non, émanant des établissements d'enseignement et de recherche français ou étrangers, des laboratoires publics ou privés.



Distributed under a Creative Commons Attribution - NonCommercial - NoDerivatives 4.0 International License

## The Get1/2 insertase forms a channel to mediate the insertion of tail-anchored proteins into the ER

### Graphical abstract



### Authors

Paul Heo, Jacob A. Culver, Jennifer Miao, Frederic Pincet, Malaiyalam Mariappan

### Correspondence

paul.heo@inserm.fr (P.H.),  
 frederic.pincet@ens.fr (F.P.),  
 malaiyalam.mariappan@yale.edu (M.M.)

### In brief

Get3 captures tail-anchored (TA) proteins and delivers them to the Get1/2 complex for ER membrane insertion. Heo et al. report that Get1/2 forms an aqueous channel that dynamically opens and closes but is sealed by Get3. Efficient insertion of TAs into the membrane depends on Get1/2 channel dynamics.

### Highlights

- The Get1/2 complex forms an aqueous channel in reconstituted lipid bilayers
- The channel is composed of two Get1/2 heterodimers with a 2.5-nm-diameter pore
- Get3 seals Get1/2 channels that dynamically open and close in the membrane
- Get1/2 channel activity is required to release TA protein from Get3 for insertion



## Article

# The Get1/2 insertase forms a channel to mediate the insertion of tail-anchored proteins into the ER

Paul Heo,<sup>1,2,\*</sup> Jacob A. Culver,<sup>3,4</sup> Jennifer Miao,<sup>3,4</sup> Frederic Pincet,<sup>1,\*</sup> and Malaiyalam Mariappan<sup>3,4,5,\*</sup><sup>1</sup>Laboratoire de Physique de l'Ecole Normale Supérieure, ENS, Université PSL, CNRS, Sorbonne Université, Université de Paris, 75005 Paris, France<sup>2</sup>Institute of Psychiatry and Neuroscience of Paris, INSERM U1266, 75014 Paris, France<sup>3</sup>Department of Cell Biology, Yale School of Medicine, 333 Cedar Street, New Haven, CT 06520, USA<sup>4</sup>Nanobiology Institute, Yale University West Campus, West Haven, CT 06516, USA<sup>5</sup>Lead contact

\*Correspondence: paul.heo@inserm.fr (P.H.), frederic.pincet@ens.fr (F.P.), malaiyalam.mariappan@yale.edu (M.M.)

<https://doi.org/10.1016/j.celrep.2022.111921>

## SUMMARY

Tail-anchored (TA) proteins contain a single C-terminal transmembrane domain (TMD) that is captured by the cytosolic Get3 in yeast (TRC40 in humans). Get3 delivers TA proteins to the Get1/2 complex for insertion into the endoplasmic reticulum (ER) membrane. How Get1/2 mediates insertion of TMDs of TA proteins into the membrane is poorly understood. Using bulk fluorescence and microfluidics assays, we show that Get1/2 forms an aqueous channel in reconstituted bilayers. We estimate the channel diameter to be  $\sim 2.5$  nm wide, corresponding to the circumference of two Get1/2 complexes. We find that the Get3 binding can seal the Get1/2 channel, which dynamically opens and closes. Our mutation analysis further shows that the Get1/2 channel activity is required to release TA proteins from Get3 for insertion into the membrane. Hence, we propose that the Get1/2 channel functions as an insertase for insertion of TMDs and as a translocase for translocation of C-terminal hydrophilic segments.

## INTRODUCTION

More than one-third of cellular mRNAs encode membrane proteins that must be selectively delivered to and inserted into the lipid bilayer of an intracellular organelle.<sup>1,2</sup> Most of these proteins are co-translationally targeted and inserted into the endoplasmic reticulum (ER). The cytosolic signal recognition particle (SRP) recognizes the first transmembrane domain (TMD) of membrane proteins and targets the ribosome-nascent chain complex to the Sec61 translocon in the ER membrane via the SRP receptor.<sup>3,4</sup> The Sec61 translocon forms an aqueous channel that recognizes an incoming TMD and facilitates its insertion into the lipid bilayer.<sup>5,6</sup> The key step in this process is thought to involve movement of a TMD from the interior aqueous pore of the Sec61 translocon into the hydrophobic core of the lipid bilayer through a lateral gate.<sup>7–9</sup> Simultaneously, the Sec61 channel can also open perpendicularly to the ER lumen to transport hydrophilic nascent polypeptides across the membrane. The quiescent Sec61 channel is closed by its plug domain, located on the luminal side of the channel, maintaining the membrane barrier.<sup>10</sup>

Recent genetic, biochemical, and structural studies have illustrated an alternative post-translational protein insertion pathway called GET (guided entry of tail-anchored proteins) in yeast and TMD recognition complex (TRC) in mammals.<sup>11–18</sup> Tail-anchored

(TA) membrane proteins are the main clients of the GET pathway. They contain a cytosolic N-terminal soluble domain and a single C-terminal TMD that serves as a membrane anchor and a targeting signal. TA proteins comprise up to 5% of the eukaryotic membrane proteome and have a wide range of important functions, including vesicle fusion, protein translocation, and lipid transport.<sup>19–21</sup> Newly synthesized TA proteins cannot utilize the co-translational SRP-mediated targeting pathway because their C-terminal TMDs remain sequestered by ribosomes when translation terminates.<sup>19,22,23</sup> The cytosolic ATPase, called Get3 in yeast (TRC40 in mammals), recognizes TMDs of TA substrates.<sup>11,12,24–26</sup> The Get3-bound TA protein complex is then recruited to the ER membrane by interaction with the long flexible Get2 cytosolic domain.<sup>27–32</sup> At the membrane, the cytosolic Get1 coiled-coil domain facilitates release of the TMD from Get3 for insertion into the lipid bilayer.<sup>32–35</sup> Subsequently, ATP binding displaces Get3 from the Get1/2 complex.<sup>27,28,33,34</sup> The Get4/5 complex also prevents rebinding of Get3 to the Get1/2 complex by sequestering the ATP-bound Get3 for another round of TA protein loading.<sup>34</sup>

Despite the molecular level of understanding of TA protein targeting to the ER membrane, the decisive final step of TA protein insertion into the ER lipid bilayer remains poorly understood.<sup>14–16,36</sup> Specifically, it is ill defined how the Get1/2 complex reduces the activation energy barrier associated with



inserting TMDs of TA proteins into the lipid bilayer. The energy barrier here is twofold. First, the hydrophobic TMD must pass hydrophilic lipid head groups of the membrane. Second, a TA protein can have a hydrophilic tail up to 30 amino acids in length<sup>37</sup> that must pass hydrophobic lipid tail groups in the membrane. Biochemical studies have revealed that the TMD of the TA substrate directly contacts the membrane domains of Get1/2 during its insertion into the ER membrane, suggesting that Get1/2 functions as an insertase.<sup>35</sup> A single-molecule *in vitro* study has shown that a heterodimer of Get1/2 is the minimum functional unit to form a TA protein insertase.<sup>32</sup> However, recent structural studies have revealed the heterotetrameric Get1/2 complex to be bound to the Get3 dimer.<sup>38</sup> Moreover, the formation of Get1/2 heterotetramers appears to be important for insertion of TA proteins into the ER of yeast cells. Interestingly, analogous to the YidC membrane protein insertase,<sup>39</sup> Get1/2 contains a cytosolic hydrophilic vestibule that has been suggested to aid insertion of TMDs of TA proteins into the bilayer.<sup>38</sup> However, it remains to be determined how the Get1/2 insertase provides a conduit for TMDs of TA proteins to enter the bilayer and allows translocation of C-terminal hydrophilic tails across the hydrophobic bilayer. Well-defined *in vitro* setups that directly monitor the dynamics of the insertion machinery on the ER membrane are required to understand the mechanisms of TA protein insertion.

To this end, we employed a combination of bulk fluorescence, microfluidics, and insertion assays to investigate the Get1/2 insertion machinery. We reveal that the reconstituted Get1/2 complex in the membrane conducts ions by forming a heterotetrameric channel that dynamically opens and closes. Our data suggest that the cytosolic binding partner Get3 seals the conductance of the Get1/2 channel, likely maintaining the membrane permeability barrier in cells. Mutagenesis studies reveal that positively charged amino acids (K150 and K157) in the first TMD of Get2 contribute to forming the Get1/2 channel. Our functional reconstitution studies show that channel formation is required to efficiently release TA substrates from Get3 for insertion into the membrane. These findings suggest that, analogous to the Sec61 translocon channel, Get1/2 functions as an insertase for inserting TMDs into the bilayer and as a translocase for translocation of hydrophilic segments across the ER membrane.

## RESULTS

### Get1/2 transports solutes in reconstituted vesicles

To test whether, like the Sec61 translocon, Get1/2 could form a channel on membranes, we used the conventional fluorescence quenching assay, in which nitro-2-1,3-benzoxadiazol-4-yl (NBD)-labeled phospholipids are quenched by sodium dithionite.<sup>40,41</sup> When NBD-conjugated lipids are present in the bilayer of small unilamellar vesicles (SUVs), only outward-facing NBD dyes are quenched by addition of the membrane-impermeable sodium dithionite. However, if the bilayer contains a channel that allows passage of sodium dithionite across the membrane, then inward- and outward-facing NBD dyes are quenched. We reconstituted purified recombinant Get1 and Get2 proteins (Figure S1A) into SUVs using a previously established procedure.<sup>42</sup>

The Get1/2 complex was efficiently incorporated into vesicles, as observed by little loss of proteins during the reconstitution procedure (Figure S1B). Digestion of SUVs with proteinase K suggest that ~18% of Get1 and Get2 were reversely oriented in the bilayer, as evidenced by the observation of protease-protected cytosolic domains of Get1 and Get2 (Figures S1C–S1E). However, it is unlikely that the remaining ~82% of Get1/2 is correctly oriented in SUVs because proteinase K would also digest uninserted Get1/2 and Get1/2 stuck on the membrane surface in addition to digesting correctly oriented Get1/2 in the membrane. As a negative control, we reconstituted a non-channel-forming membrane protein, either tSNARE (target soluble N-ethylmaleimide-sensitive factor attachment protein receptor) or vesicle-associated vSNARE, into SUVs (Figures 1A and S1F).<sup>43</sup> To serve as a positive control for channel formation, we reconstituted the heptameric toxin  $\alpha$ -hemolysin into SUVs.<sup>44</sup>

Upon addition of sodium dithionite, the NBD fluorescence reduction was monitored on a plate reader. The relative fluorescence decrease is a direct quantification of all NBD-labeled lipids accessible to the sodium dithionite. We found that the fluorescence of protein-free SUVs was reduced to ~40% of the initial NBD fluorescence (Figure 1B). This result is consistent with immediate quenching of all NBD fluorophores localized on the outer leaflet, whereas the inner leaflet is not quenched because sodium dithionite cannot penetrate the SUVs (Figures 1A and 1B). We obtained a similar result with SUVs containing tSNARE or vSNARE, which is consistent with the observation that SNAREs do not form channels.<sup>43</sup> Because the bacterial toxin hemolysin is known to form an oligomeric channel,<sup>43</sup> the fluorescence was further reduced to ~33% for H2000 SUVs containing an  $\alpha$ -hemolysin-to-lipid ratio of 1:2,000 and reduced to ~25% for H500 SUVs having an  $\alpha$ -hemolysin-to-lipid ratio of 1:500 (Figure 1B). These results confirm that the inner leaflet of SUVs is quenched by sodium dithionite only in the presence of a membrane protein channel. Remarkably, the fluorescence of Get1/2 SUVs with a protein-to-lipid ratio of 1:3,500 was significantly reduced to ~13% (Figure 1B). This result suggests that sodium dithionite passes through the Get1/2-containing membrane bilayer and that, like  $\alpha$ -hemolysin, Get1/2 complexes can form membrane channels. It is intriguing that the fluorescence plateau is not reaching zero for  $\alpha$ -hemolysin or Get1/2 samples. This non-zero plateau shows that some SUVs are not permeable to dithionite, suggesting that they may not have any channel (Figure S2; STAR Methods). A final striking result is that, after the sharp fluorescence decrease upon adding sodium dithionite, the fluorescence signal remained constant for protein-free and  $\alpha$ -hemolysin samples. In contrast, the NBD fluorescence of Get1/2 SUVs continued to decrease for 40 min until reaching the plateau value (Figure 1B). This shows that some SUVs are initially not permeable but become permeable over time, suggesting that the Get1/2 channels are transient.

### Get1/2-induced membrane permeability is caused by transient channels

The aforementioned fluorescence quenching experiments in bulk suggest that Get1/2 can form a transient channel that allows passage of solutes like sodium dithionite. To characterize the individual Get1/2 channel, we employed our recently developed

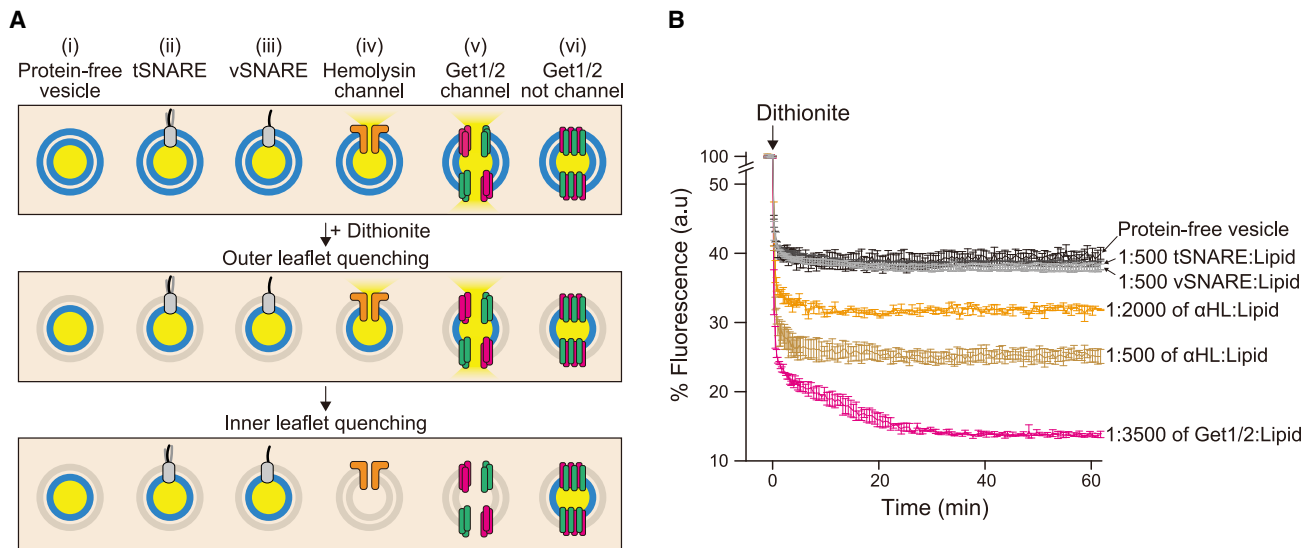


**Figure 1. The Get1/2 complex makes membranes permeable to solutes**

(A) Description of the 6 SUV samples used and the expected outcome of the bulk fluorescence quenching experiment.

(B) NBD fluorescence was monitored over 60 min for the indicated samples. 1 mM sodium dithionite is added to SUVs at  $t = 0$ . The lipid-to-protein ratio was defined when they were mixed for setting up reconstitution reactions.

Data represent an average of three independent experiments (except for the H2000 sample in which there were two independent experiments). Error bars indicate mean  $\pm$  SD. See also [Figures S1](#).

*in vitro* reconstituted system in which a free-standing membrane ( $\sim 100 \mu\text{m}$  in diameter) is suspended between two microfluidics channels ([Figure 2A](#)).<sup>43</sup> We flowed protein-free SUVs on the bottom microfluidics channel and Get1/2 decorated SUVs (Get1/2:lipid ratio of 1:3,500) on the top microfluidics channel. A suspended squalene droplet was trapped between the two microfluidics channels. This results in formation of a Get1/2-containing leaflet on the top side and a protein-free leaflet on the bottom side of the squalene droplet. Upon absorption of squalene by polydimethylsiloxane (PDMS), the two leaflets contact and zip to form a bilayer ([Figure 2A](#)). Because the Get1/2 complex is inserted in a single leaflet at the buffer/squalene interface, it is energetically favorable to insert with the hydrophilic cytosolic domains facing the buffer. Membrane formation was simultaneously monitored by microscope and patch amplifier ([Figure 2A](#)).

We measured current through the membrane by applying a permanent 100-mV voltage difference between the upper and lower channels. The membranes exhibited stable readings for  $\sim 4$  h, after which there is no resistance for the current because of breakage of the membrane. As expected, absolutely no current was observed in the case of the protein-free membrane for 4 h ([Figure 2B](#)). In contrast, in the case of Get1/2 membranes, spikes of current jumps were observed, indicating that channels are forming, allowing ions to cross the membrane ([Figures 2C](#), [2D](#), and [S3](#)). The current was not permanently occurring, but instead it exhibited stepwise increases and decreases until returning to zero. These observations suggest that transient Get1/2 channels stochastically form in the membrane. Most of these current steps were close to 60 pA, but some of them were larger. We also observed that channels formed for long pe-

riods of time without any current alternating for various durations (a few seconds to tens of minutes), during which currents remained non-zero (or only briefly became zero). On average, these cascades of transient channels occurred  $\sim 4$ –5 times per hour and existed 15% of the time, which means that they lasted  $\sim 2$  min on average. However, this average is not a perfect representation because a “cascade” may actually be represented by a single brief channel opening (0.3 s in [Figure 2D](#), left panel) or by a long series of opening and closing of several channels that can last for many minutes ([Figure 2D](#), right panel).

### The channel is made by two Get1/2 complexes

The current plateaus represent the inner diameter of a single channel and the number of channels simultaneously opened in the membrane. We analyzed 301 current plateaus from four independent membranes suspended in microfluidics chips that were measured for a combined total of more than 12 h. Most plateaus are found at around 60 pA ([Figure 2D](#)). We also noticed that the smallest plateau above the detection limit is at 20 pA ([Figure 2E](#)), which is sometimes step increased to the typical distinct plateau around 60 pA. The current distribution of the 301 plateaus does not clearly display two distinct peaks around 20 and 60 pA. This is probably due to the intrinsic noise of the experiment. An alternate analysis is to investigate sudden stepwise increases and decreases. This approach removes any discrepancy because of variable background. We analyzed 194 current step increases and 208 current step decreases. The corresponding histograms are provided in [Figures 3A](#) and [3B](#). Four “peaks” associated with four groups of stepwise current variations and having mean values of  $\sim 124$  pA, 184 pA, 250 pA, and 308 pA can be observed (peaks 3, 4, 5, and 6, respectively, in [Figure 3A](#)).

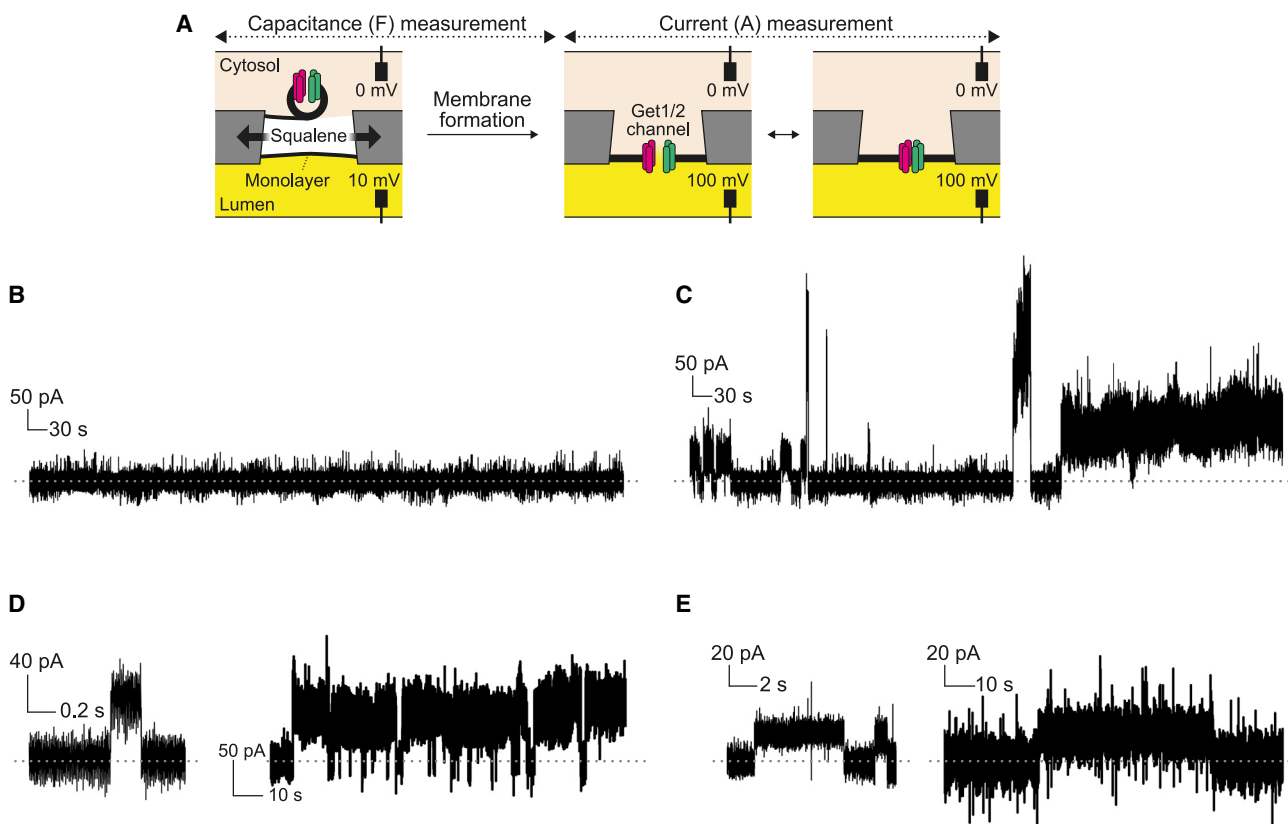


**Figure 2. Get1/2 channel formation in a free-floating membrane**

(A) A schematic of the experimental setup. A free-floating membrane is suspended between two microfluidics channels, as described in the text and STAR Methods.

(B) No current is observed in protein-free membranes until their rupture.

(C) In Get1/2-decorated membranes, transient currents are typically observed in sequential increases and decreases. These currents attest to the presence of channels in the membrane through which ions can pass upon the action of the voltage applied on the two sides of the membrane. This step increase and decrease of currents shows that the channels are very dynamic and can open and close. The data were collected from four independent experiments.

(D) Magnification of traces. The left panel shows a channel that opens and reseals in less than 0.5 s. The right panel shows a channel that is intermittently opened and closed for 100 s (the duration of an acquisition trace is 1,000 s; hence, this channel did not reseal by the end of the trace).

(E) Examples of 20-pA currents. Left panel: a channel corresponding to a 20-pA current is opened and closed twice in less than 10 s. Right panel: a 20-pA channel remains open for almost a minute, and a transient 60- to 70-pA channel briefly opens during the process on the current trace.

See also Figures S2 and S3.

The increase in current between each successive peak seems constant and close to 60 pA. Based on the observation that there are 20-pA and 60-pA plateaus, we fitted the smallest current steps, including peak 3, with three Gaussians (Figure 3B). We found the position of the corresponding peaks at 19.6 pA, 55.2 pA, and 123.9 pA (peaks 1, 2, and 3, respectively, in Figures 3A and 3B). The large error bar on the second peak is due to the proximity to the first peak.

Two models can be envisioned to explain these stepwise variations of the current. First, the change in current is due to opening or closing of pores of a unique size. Second, pores can change their size by adding or removing Get1/2 complexes. The two models can be discriminated by plotting the conductance versus the associated peak number. In the case of a single channel with increasing size, the conductance varies with the square of the peak number because the channel area increases with the square of the channel circumference. In the case of

opening of new channels of fixed size, the conductance varies linearly because the total channel area is proportional to the number of channels. For Get1/2, the conductance variation is clearly linear with the peak number (Figure 3C) from peaks 3–6. Peak 2, obtained by fitting the smallest current steps, also falls on the same line. This result suggests that Get1/2 forms channels of precise conductance (i.e., of precise size), and the subsequent current plateaus correspond to various numbers of identical channels that opened simultaneously.

The slope indicates a conductance increase of 0.6 nS per channel (Figure 3C). This is about 5 times that of an  $\alpha$ -hemolysin channel we measured with the same membrane (0.125 nS). The conductance is proportional to  $A/l$ , where  $A$  and  $l$  are the channel inner area and length, respectively. For  $\alpha$ -hemolysin,  $A$  is  $1.8\text{ nm}^2$ , and  $l$  is 10 nm. The length of the Get1/2 channel will be longer than a lipid bilayer (4 nm). The luminal loops and extremities of Get1 and Get2 are rather short, suggesting that a



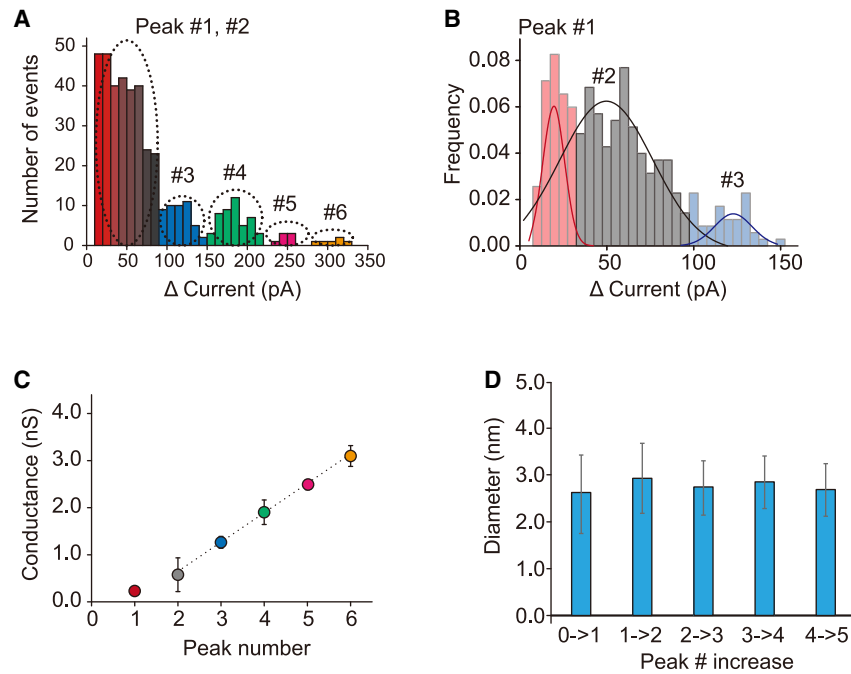


**Figure 3. Conductance of a single Get1/2 channel**

(A) Current step increases and decreases from all four independent experiments are pooled and presented in a histogram with 10-pA bins from 0–350 pA. The positions of the peaks in the distribution are highlighted by dashed circles. Peak 1 is highlighted in red because it corresponds to an intermediate incomplete Get1/2 channel (see text for explanation). Peaks 2–6 correspond, respectively, to current steps in which 1, 2, 3, 4, and 5 Get1/2 channels are opening or closing simultaneously (increase or decrease as observed in Figures 2C–2E). (B) The same distribution presented between 0 pA and 150 pA with 5 pA bins. The histogram is fitted with Origin software by 3 Gaussian peaks that are used to determine the position of peaks 1–3. The positions of peaks 4–6 in A are estimated by averaging the current step values in the corresponding current range. (C) Variation of the conductance with the peak number was calculated from four independent experiments. Error bars indicate mean  $\pm$  SD. The conductance is the ratio between the peak current and 100-mV voltage applied between the two channels. Peaks 2–6 are perfectly aligned. The corresponding fit is presented in the figure. Peak 1 is not aligned with the others. This shows that each peak from 2–6 corresponds to addition of an identical Get1/2 channel.

(D) The mean diameter of the additional channel observed between two consecutive peaks is calculated from the conductance variation data collected from four independent experiments. Error bars indicate mean  $\pm$  SD. As expected, there is no significant difference between the various increases, as indicated in the text. See also Figures S4.

channel cannot extend significantly into the ER lumen. The cytoplasmic loops have a length of 83 and 47 residues for Get1 and Get2, respectively. The cytoplasmic C-terminal of Get1 is 36 residues and the cytoplasmic N-terminal of Get2 is 147 residues. Apart from these aforementioned loops, the other loops and tails are short in Get1 and Get2. Hence, it is reasonable to assume that the channel will not extend much in the cytoplasm: 4–10 nm for the Get1/2 channel length is a probable estimate. Using the geometrical parameters of  $\alpha$ -hemolysin, this indicates that the inner area of the Get1/2 channel is 3.6–9 nm<sup>2</sup>; i.e. equivalent to a disk with a diameter of 2.1–3.4 nm (Figure 3D). This is consistent with the inner area of a channel formed by 12 1-nm transmembrane  $\alpha$  helices forming a dodecamer; i.e., two Get1/2 complexes (Figure S4; STAR Methods). However, we have to be cautious because this calculation assumes a perfectly cylindrical channel. Hence, we cannot exclude the possibility that the channel is made of a single Get1/2 complex because a hexamer of six 1.3-nm  $\alpha$ -helices would form a perfectly cylindrical channel with a 1.7-nm<sup>2</sup> open cross-section, which is still in a reasonable range. Three Get1/2 complexes per channel cannot be envisioned because an octadecagon made of 18 1-nm  $\alpha$  helices would form a perfectly cylindrical channel with a 46-nm<sup>2</sup> open cross-section, which is much larger than we measured (Figure S4; STAR Methods). Intriguingly, the conductance of the first peak is not aligned with the others (Figure 3C). Also, the intercept with  $y = 0$  axis is exactly at  $x = 1$ . This suggests that the channel in the first peak is not of the same nature as the others. Because it often precedes or follows a 60-pA plateau, it is probably an intermediate state that sometimes forms during channel formation or closing. This intermediate state has a

conductance corresponding to an  $\sim$ 1.4-nm diameter, which could correspond to a single Get1/2 complex that may form a small channel on the pathway to full channel formation or closing. We do not observe this intermediate state systematically, either because it may not always occur or because it is too short lived or too close to our detection limit.

### Characterization of the Get1/2 channel

The data above suggest that Get1/2 forms a hydrophilic channel with a diameter of between 2.1 and 3.4 nm. If this estimation is the threshold of the pore size, smaller or bigger molecules should pass through or be blocked by the membrane, respectively. To test this, we used a conventional content release assay in which GFP ( $\sim$ 3-nm diameter)<sup>45</sup> or sulforhodamine B (SRB;  $\sim$ 1-nm diameter) is encapsulated in the desired SUVs (Figure 4A). GFP was not released from Get1/2 SUVs, as evidenced by encapsulated GFP fluorescence not reducing in the presence of the Get1/2 channel (Figure 4B). Conversely, the SRB fluorescence was reduced to  $\sim$ 50% for SUVs containing a Get1/2-to-lipid ratio of 1:3,500 and about  $\sim$ 35% for SUVs having a Get1/2 to lipid ratio of 1:7,000 (Figure 4C). The electric measurements combined with the dye release suggest that the Get1/2 channel pore size is  $2.5 \pm 0.4$  nm.

To characterize the Get1/2 channel, we sought to identify mutations in Get1/2 that would disrupt the channel activity. Recent structural studies suggest that two lysine residues (K150 and K157) in Get2 TMD1 mediate heterotetramerization of Get1/2 by binding to phosphatidylinositol (PI).<sup>38</sup> We hypothesized that mutating K150 and K157 in Get2 TMD1 to alanine residues should disrupt the channel activity by inhibiting

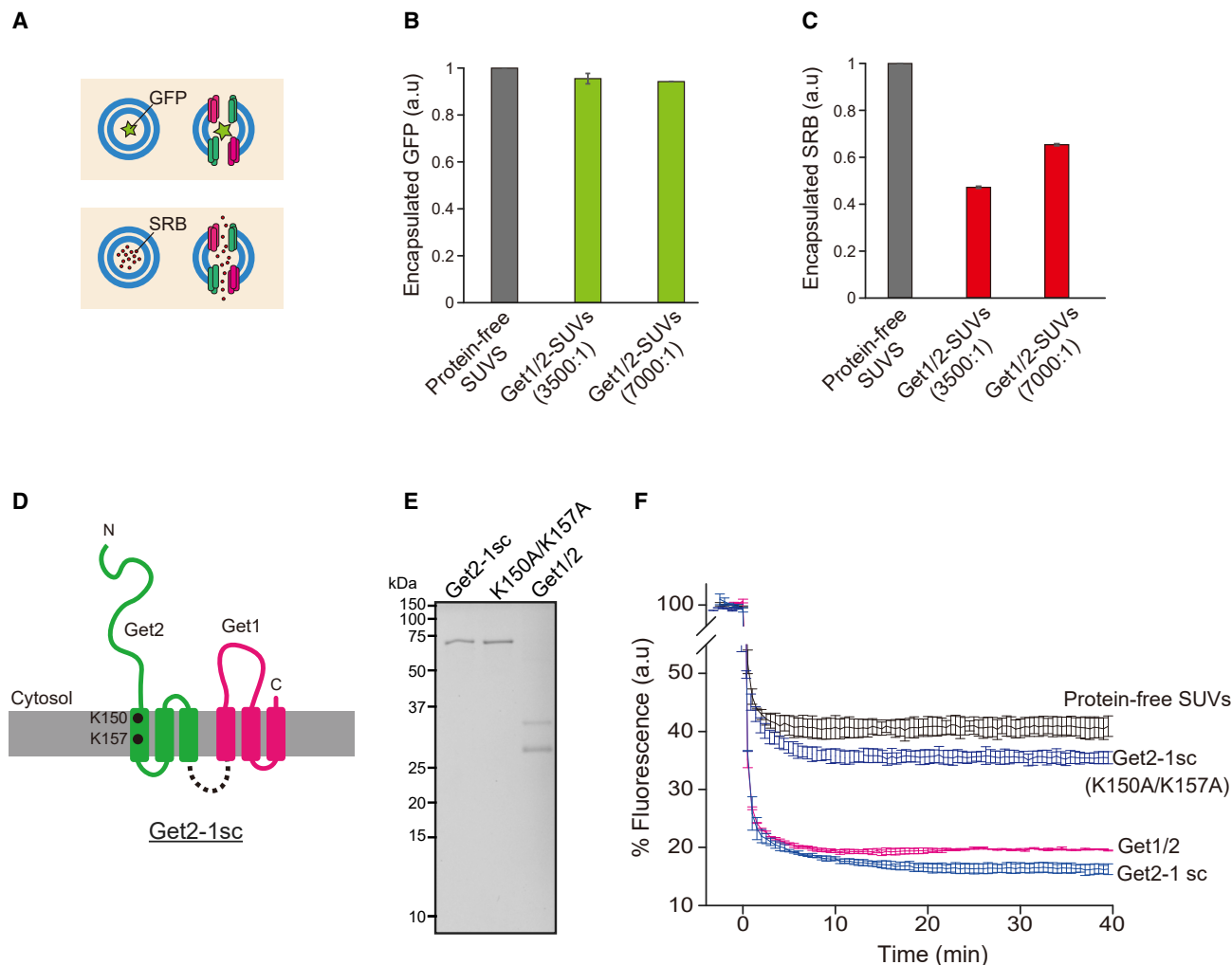


**Figure 4. Get1/2 forms a heterotetrameric channel with a defined pore size**

(A) Schematic showing GFP or SRB encapsulated in Get1/2 SUVs.

(B and C) GFP or SRB was encapsulated in protein-free SUVs or Get1/2 SUVs with the indicated lipid-to-protein ratio. The retained fluorescence of GFP or SRB was quantified after removal of exterior free dyes. Data represent an average of two independent experiments. Error bars represent mean  $\pm$  SD.

(D) Diagram illustrating the topology of the Get2-1sc. K150 and K157 in Get2 TMD1 were mutated to alanine residues. The dotted line indicates the linker sequence that connects the C terminus of Get2 to the N terminus of Get1.

(E) The indicated SUVs were analyzed by Coomassie staining.

(F) NBD fluorescence was monitored for 40 min for the indicated samples. 1 mM sodium dithionite is added to SUVs at  $t = 0$ .

Data represent an average of two independent experiments. Error bars represent mean  $\pm$  SD. See also [Figures S5](#) and [S6](#).

heterotetramerization of Get1/2. To exclude the potential for complex disruption by these mutations, we introduced K150A and K157A mutations into Get2 of the single-chain (sc) Get2-1 construct (Figure 4D), which is known to be functional *in vitro* and in yeast<sup>32,35</sup> (Figure 1A). We individually expressed wild-type Get2-1sc and Get2-1sc (K150A/K157A) and purified them from *E. coli* (Figure S5A). We then reconstituted wild-type (WT) or mutant Get2-1sc into SUVs and carried out a fluorescence quenching assay, shown in Figure 1B. Similar to Get1/2 SUVs, ~80% of Get2-1sc or ~93% of Get2-1sc (K150A/K157A) is correctly oriented in SUVs, as judged by a proteinase protection assay (Figures S5B–S5D). Upon adding sodium dithionite, the fluorescence of SUVs containing Get1/2 or Get2-1sc was

reduced to ~20% of the initial NBD fluorescence (Figures 4E and 4F). In sharp contrast, the fluorescence of SUVs containing Get2-1sc (K150A/K157A) was only reduced to 40%, similar to that of protein-free SUVs, demonstrating that the two lysine residues in TMD1 of Get2 contribute to Get1/2 channel formation. Because earlier studies suggested that the K150 and K157 residues in Get2 mediate formation of Get1/2 heterotetramers by binding to PI, we examined this by performing chemical crosslinking using a lysine-reactive chemical crosslinker. To our surprise, proteoliposomes containing Get2-1sc or Get2-1sc (K150A/K157A) showed a similar level of crosslinked adduct corresponding to the size of heterotetramers even at the various protein or crosslinker concentrations (Figures S6A and S6B). A



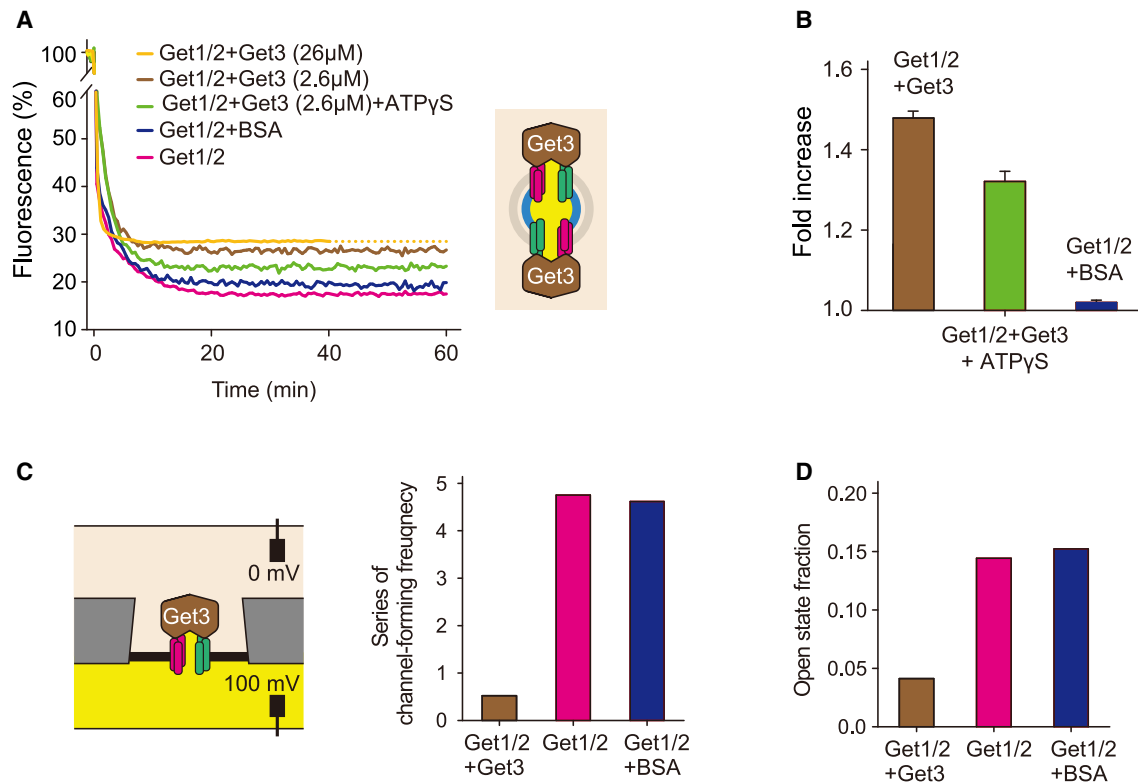


**Figure 5. Get3 seals the Get1/2 channel**

(A) Example of an NBD quenching assay similar to that presented in Figure 1. 2.6  $\mu$ M or 26  $\mu$ M Get3 was incubated with Get1/2 SUVs in the presence or absence of 1 mM ATP $\gamma$ S/MgCl<sub>2</sub>. As a negative control, 5  $\mu$ M BSA was incubated with Get1/2 SUVs. NBD fluorescence quenching in the inner leaflet is reduced as the concentration of Get3 is increased. The dotted line indicates the guideline for Get1/2 + Get3 (26  $\mu$ M). The experiment was repeated independently three times with less than 5% variation.

(B) Mean relative increase of the fluorescence plateau in (A) as the ratio between the plateau of the considered conditions to that of the reference quenching obtained with Get1/2 alone (pink curve). Data represent an average of three independent experiments. Error bars represent mean  $\pm$  SD.

(C) Comparison of the frequency of the Get1/2 channel series in microfluidics experiments similar to that presented in Figure 2 but performed with Get3 or BSA flow in the top channel. This frequency is decreased 10-fold with Get3 but not with BSA.

(D) Comparison of the fraction of the time a Get1/2 channel series in microfluidics experiments similar to that presented in Figure 2, but Get3 or BSA was flowed in the top channel. This fraction is decreased  $\sim$ 4-fold with Get3 but not with BSA. The experiments shown in Figures 3C and 3D were repeated three times with similar results.

small fraction of Get2-1sc or its mutant could form a crosslinked adduct corresponding to hetero-octamers, which suggests that the heterotetrameric channels can transiently associate with themselves. It is unclear why these mutations did not disrupt heterotetramerization of Get1/2, as suggested previously, but we provide possible explanations for this discrepancy in the Discussion.

### Get3 seals the Get1/2 channel

Because the Get1/2 channel allows passage of small molecules, we wanted to determine how the ER membrane permeability barrier is maintained to prevent the deleterious effects caused by exchange of small molecules between the ER and cytosol. We hypothesized that the cytosolic binding partner Get3 might regulate channel opening because earlier studies have shown that Get3 is localized on the ER membrane in yeast and forms a tight complex with Get1 and Get2.<sup>11,27</sup> To investigate this hypothesis, we first measured fluorescence quenching in bulk

experiments using Get1/2 SUVs in the absence or presence of 2.6  $\mu$ M Get3, which corresponds to  $\sim$ 300 per Get1/2 complex (Figure 5A). The NBD fluorescence plateau reached  $\sim$ 30% of the initial fluorescence in the presence of Get3 (Figure 5A). This value, when compared with  $\sim$ 15%–20% for Get1/2-only SUVs (Figures 1D and 5A), indicates that inner leaflet NBD quenching was reduced by approximately half when Get3 was added, i.e., about half of the porous vesicles were resealed by Get3. A 10-fold increase in the concentration of Get3 (26  $\mu$ M) did not significantly enhance sealing of the Get1/2 channel, suggesting that Get3 is not limited in this experiment (Figure 5A). Two plausible explanations follow for why Get3 does not fully close the Get1/2 channel. First, about 18% of the Get1/2 complexes cannot bind to Get3 because they are in the reverse orientation (Figures S1C–S1E). Second, Get3 binding may restrict but not completely block leakage of sodium dithionite through the channel. Get3 binding and sealing the Get1/2 channel are specific because we did not observe any difference between Get1/2

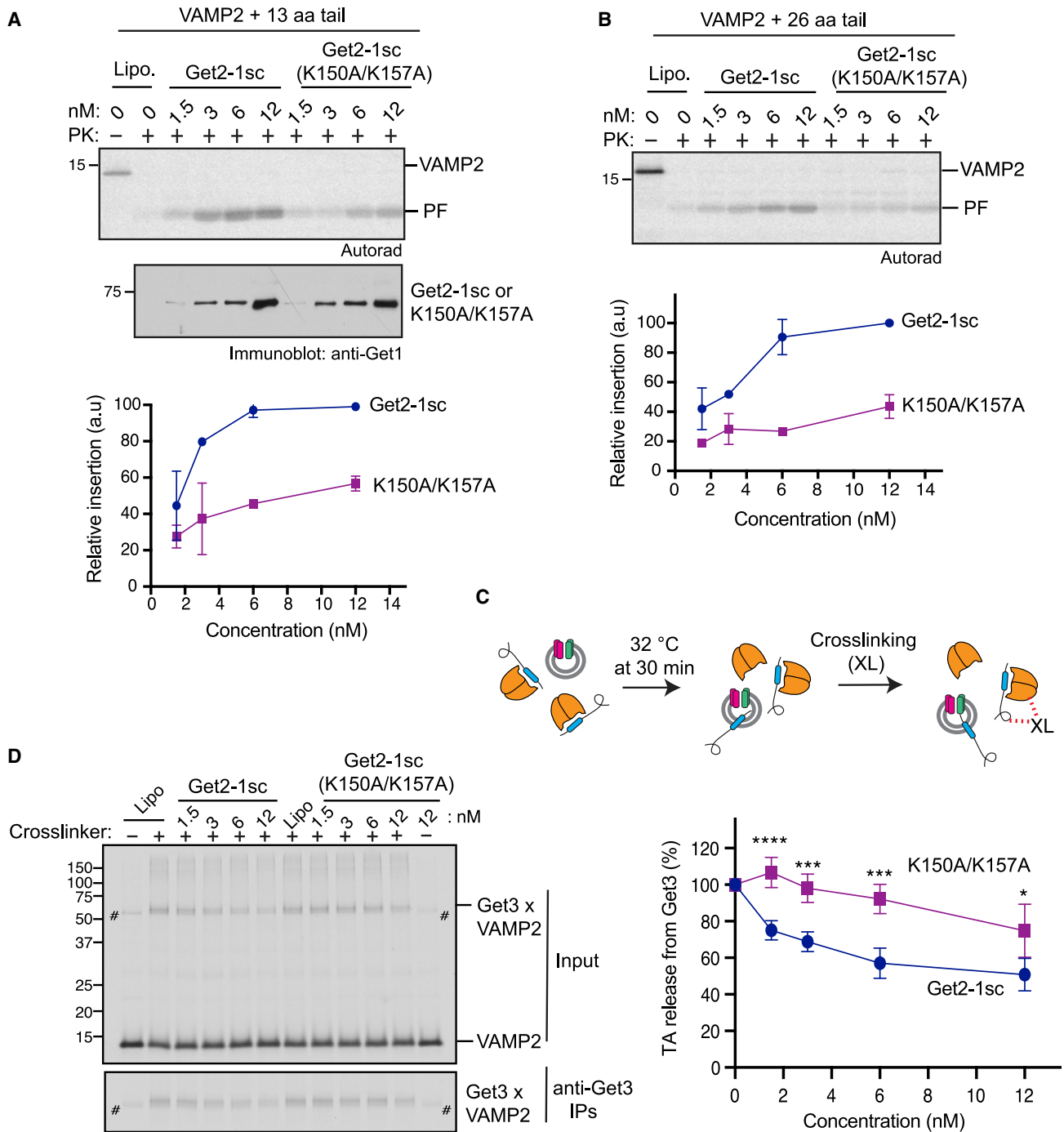


**Figure 6. Get1/2 channel mediates TA protein insertion**

(A) Protein-free, Get2-1sc, or Get2-1sc (K150A/K157A) liposomes were incubated with the purified complex of Get3 and VAMP2 with a 13-amino-acid C-terminal tail. The proteinase K (PK)-protected fragment (PF) represents successful insertion. Proteoliposomes used for the TA protein insertion assay were analyzed by immunoblotting with anti-Get2 antibodies. Bottom: TA protein insertion was quantified by autoradiography. Data represent an average of two independent experiments. Error bars represent mean  $\pm$  SD.

(B) TA protein insertion and quantification were conducted as in (A) but using the purified complex of Get3 and VAMP2 bearing a 26-amino-acid C-terminal hydrophilic tail. Data represent an average of two independent experiments. Error bars represent mean  $\pm$  SD.

(C) Schematic of the TA protein release assay.

(legend continued on next page)

SUVs with and without bovine serum albumin (BSA). Earlier studies suggest that ADP-bound Get3 binds tightly to Get1/2, whereas Get3 is released from Get1/2 when bound to ATP.<sup>27,28,33,34</sup> We therefore investigated how ATP binding to Get3 affects NBD quenching mediated by Get1/2 channels using bulk experiments in the presence of the ATP analog ATP $\gamma$ S, which cannot be hydrolyzed. We found that the fluorescence plateau during dequenching reached  $\sim$ 25% of the initial fluorescence, suggesting that the membrane's impermeability to solutes is reduced when Get3 is bound to ATP $\gamma$ S (Figure 5B). Overall, the number of liposomes having their membrane sealed by Get3 was reduced by about one-third.

We turned to our microfluidics experiments to further support Get3-mediated sealing of the Get1/2 channel. Using 100 nM Get3, we observed only three series of channels formed in three different experiments for a total duration of almost 6 h, corresponding to the frequency (0.5 per hour) of 10 times less than without Get3 (Figure 5C). Overall, a channel was opened 4% of the time with Get3 versus 15% without Get3 (Figure 5C). The average duration of a series of channels cannot be accurately obtained over such a low number of events but remains in the same range as the one observed without Get3 (4.5 min versus 2 min). This result suggests that Get3 either binds and seals a channel or does not bind at all, which could be partially explained by a population of channels that are reversely oriented and uninserted. As a control, we replaced Get3 with BSA at 100 nM (2 experiments for 6 h). We did not observe any difference between samples with and without BSA (Figures 5C and 5D). Our functional studies at the bulk and single-channel levels provide evidence that Get3, without TA protein cargo, seals Get1/2 channels and prevents solute exchange across the membrane. These studies also provided information about the interaction between Get1/2 and Get3. Because a quenching reduction can be seen in the bulk experiment when the Get3 concentration is 2.6  $\mu$ M and, to a lesser extent, at a concentration of 260 nM, the affinity of Get3 to Get1/2 is of the order of 100 nM to 1  $\mu$ M. This is consistent with the significant reduction of channel opening in the microfluidics channel in the presence of Get3 at 100 nM.

### Efficient insertion of TA proteins relies on Get1/2 channel activity

We hypothesized that formation of the Get1/2 channel might be required for mediating insertion of TA proteins into the ER membrane. To test this, we assembled and affinity-purified Get3 bound to radiolabeled VAMP2 (a SNARE TA protein that mediates fusion of synaptic vesicles) from *in vitro* translation reactions.<sup>27</sup> We then incubated the Get3-VAMP2 targeting complex with various concentrations of Get2-1sc or Get2-1sc (K150A/K157A) containing proteoliposomes and performed a protease protection assay. Protease-protected fragments of VAMP2, which represent successful insertion, were recovered

by immunoprecipitation using antibodies against its C-terminal epitope. VAMP2 was inserted into Get2-1sc proteoliposomes, and the insertion efficiency depended on the concentration of Get2-1sc (Figure 6A). In contrast, VAMP2 insertion into proteoliposomes containing Get2-1sc (K150A/K157A) was inefficient at all concentrations tested. Our data are consistent with the previous observation that the TA protein Sed5 was mislocalized in yeast cells expressing Get2-1sc (K150A/K157A).<sup>38</sup> We reasoned that Get1/2 channel activity might be more critical for mediating insertion of TA proteins with longer C-terminal hydrophilic tails. Therefore, we prepared a targeting complex containing VAMP2 with the extended C terminus of 26 amino acids and tested for insertion into proteoliposomes containing WT or Get2-1sc mutant. Insertion of VAMP2 showed a significant reduction in K150A/K157A proteoliposomes compared with the WT (Figure 6B), but the difference was similar to that observed for VAMP2 with a short tail (Figure 6A). These results indicated that the insertion defect of Get2-1sc (K150A/K157A) may be caused by failure to recruit the targeting complex to the membrane or inability to release TA proteins from Get3. The membrane flotation assay revealed that the WT and the mutant could recruit the Get3-VAMP2 targeting complex to the bilayer (Figure S7). We next examined TA substrate release from Get3 in the presence of Get2-1sc or Get2-1sc (K150A/K157A) proteoliposomes using a chemical crosslinking assay (Figure 6C). Get2-1sc proteoliposomes stimulated VAMP2 release from Get3, as evidenced by reduced crosslinking between Get3 and VAMP2 even at low concentrations of Get2-1sc (Figure 6D). In contrast, Get2-1sc (K150A/K157A) exhibited a significant defect in releasing VAMP2 from Get3 (Figure 6D), which supports the notion that Get1/2 channel activity is required for release of TA substrates from Get3.

### DISCUSSION

This study provides evidence that the conserved TA protein insertion machinery Get1/2 forms a hydrophilic channel in the lipid bilayer. In this discussion, we focus on the stability of the Get1/2 channel, the cooperativity of multiple Get1/2 channels, and how opening of the Get1/2 channel is coupled with TA protein release from Get3 for efficient insertion into the ER membrane (Figure 7).

#### Stability of the channel: Closing rate

Spontaneous closing of a channel is an indication that a Get1/2 complex changes conformation. Because there is a series of opening/closing events, Get1 and Get2 likely remain bound to each other during these events. We hypothesize that spontaneous opening and closing of the Get1/2 channel may also accelerate the movement of Get1 and Get2 cytosolic domains, particularly the Get1 coiled coil, which is tightly connected to

(D) The Get3-VAMP2 complex was incubated with liposomes or proteoliposomes containing the indicated concentration of proteins and subjected to chemical crosslinking and immunoprecipitation with anti-Get3 antibodies. Aliquots of total crosslinking reactions (input) and immunoprecipitation products of the crosslinking reactions were analyzed by autoradiography. The right panel shows the quantification result of TA protein release from Get3.

Data represent an average of five independent experiments. Error bars represent mean  $\pm$  SD. Statistical analysis of the difference between WT and K150A/K157A for each concentration was performed using an unpaired t test. ns, not significant. \* $p < 0.05$ , \*\* $p < 0.01$ , \*\*\* $p < 0.001$ , \*\*\*\* $p < 0.0001$ . #, a background crosslinked band. See also Figure S7.

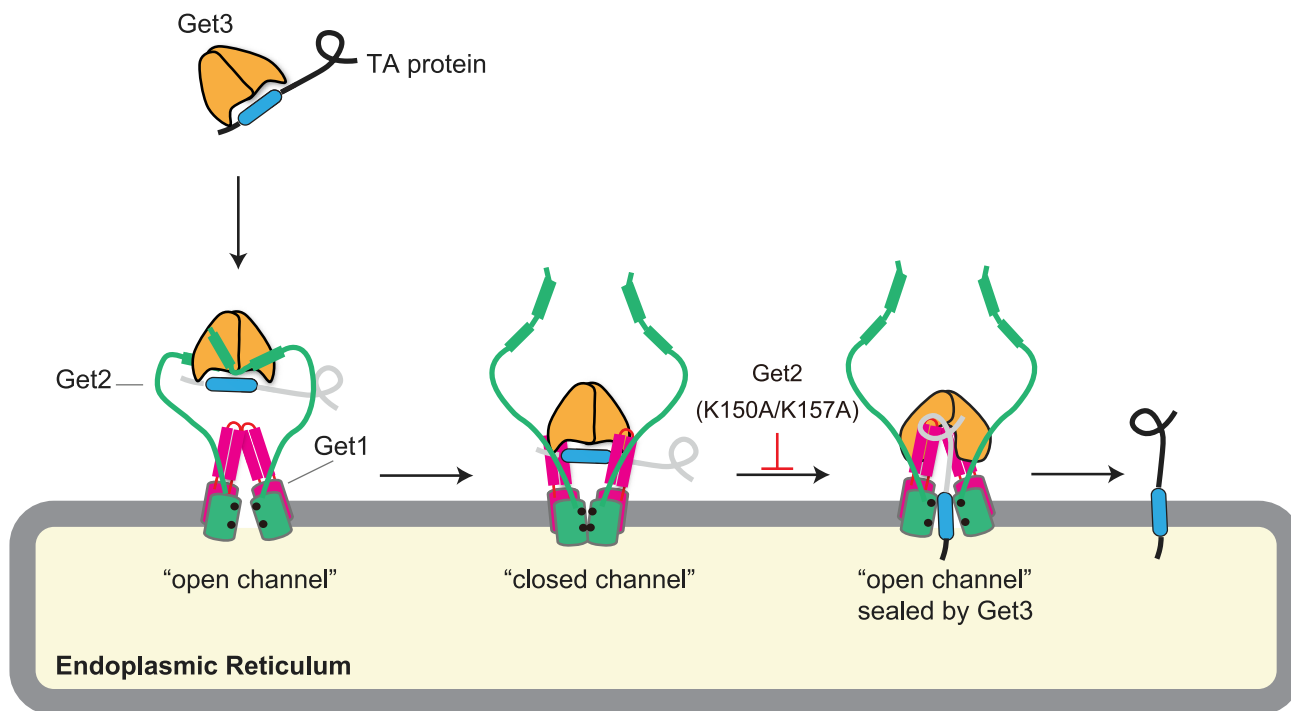


**Figure 7. Model of TA protein insertion by the Get1/2 channel**

Get1/2 forms a heterotetrameric channel that transiently opens and closes. The long and flexible cytosolic domain of Get2 recruits the Get3-TA protein complex closer to the cytosolic domain of Get1. Get1/2 channel opening and closing in the membrane accelerate the movement of the cytosolic Get1 domain to bind and release TA substrate from Get3, allowing the substrate to land directly on the channel for insertion into the ER membrane. K150A/K157A mutations in Get2 close the channel, immobilizing the Get1 coiled-coil domain, inhibiting release of TA substrate from Get3. When the TA protein is inserted into the membrane, Get3 binding to Get1/2 seals the channel until it is released by binding to ATP.

its membrane domain (Figure 7).<sup>27,38</sup> Another advantage of spontaneous closing is preventing perforation of the ER membrane, which would be physiologically damaging. Spontaneous closing of the Get1/2 channel in the absence of Get3 may be due to the low hydrophilicity of the inside channel region that is exposed to the aqueous phase, but the other side faces the hydrophobic acyl chains in the membranes. Quantitatively, this should translate into the low resealing energy of the channel. This energy can be estimated by analyzing the statistics of the channel lifetime. By pooling all experiments, channels were open for slightly more than 2 h. During these 2 h, 185 channel closing events were observed. Hence, the closing rate,  $k_{off}$ , is about 0.03 per second; i.e., a channel is stable for  $\sim 30$  s. We can estimate the energy required for the conformation change assuming a standard Arrhenius dependency of the closing rate  $k_{off} = \frac{e^{-E_b}}{\tau_0}$ , where  $E_b$  is the energy barrier for the conformation change expressed in  $k_B T$ , and  $\tau_0$  is a prefactor related to the shape of the energy landscape and the local viscosity. For nanometer-size proteins,  $\tau_0$  is between 0.1 ns and 10 ns. Hence,  $E_b = 24 \pm 3 k_B T$ . If Get3 added  $5 k_B T$  to this value, then the Get1/2 channel would become stable for more than 1 h; i.e., it would remain permanently open or closed but sealed by Get3 on the typical timescale of the cell. Conversely, if we destabilize the channel by removing as little as  $5 k_B T$ , then the average lifetime of the Get1/2 channel would be reduced to 200 ms, and the ER membrane would be protected from perforation.

Hence,  $24 \pm 3 k_B T$  is ideal to keep the channel relatively stable (30 s) and make it permanently closed or permanently open upon Get3 binding.

We speculate that the Get3-mediated sealing of the transiently opened Get1/2 channel is physiologically crucial for maintaining the membrane permeability barrier *in vivo*. We show that Get3-mediated sealing of the Get1/2 channel can be partially released in the presence of a non-hydrolyzable ATP. In addition to binding to ATP, complete release of Get3 from Get1/2 likely requires association with Get4/5.<sup>34</sup> Alternatively, ATP-bound Get3 is loosely attached to the Get1/2 channel until arrival of the Get3-TA protein complex, which may have a higher affinity to displace ATP-bound Get3 from the channel. The sealing function of Get3 would explain why the endogenous Get3 is always associated with Get1/2 and highly enriched at the ER membrane in yeast cells.<sup>11,27,46,47</sup>

#### Several channels can open and close cooperatively

270 of the 355 current steps in peaks 2–6 (170 opening events and 185 closing events) correspond to a single channel (Figure 3A). However, the remaining 85 steps correspond to several channels (up to 6) opening or closing simultaneously. This points to direct interactions between a few Get1/2 channels, which is partly supported by observation of Get1/2 crosslinked adducts larger than heterotetramers (Figure S6). In our *in vitro* setup, the most likely explanation is that these individual channels are

bound to each other and are forming a group of channels sensitive to the open or close state of the other channels in the group. Alternate explanations are unlikely because randomly distributed channels are too far apart to directly interact in the large surface area of the membrane, 10,000  $\mu\text{m}^2$ . Hence, we hypothesize that clusters composed of a few Get1/2 complexes stochastically and sometimes cooperatively form channels. With the conditions we used, these clusters form every  $\sim 15$  min and last for  $\sim 2$  min on average. However, it remains to be determined whether such clusters exist *in vivo*.

### The Get1/2 channel forms at the heterotetramer interface

Our channel recording and chemical crosslinking data suggest that two heterodimers of Get1/2 form the channel. The mutation studies suggest that the two lysine residues (K150 and K157 in Get2 TMD1) localized in the interface of Get1/2 heterotetramer<sup>38</sup> contribute to formation of a hydrophilic pore. The presented data suggest that the Get1/2 channel opens and closes dynamically but that it is permanently closed when the pore-forming K150 and K157 residues are mutated to hydrophobic alanine residues. These mutations likely enhance the hydrophobic interactions between the TMDs, closing the Get1/2 channel permanently. The same K150 and K157 residues that contribute to channel formation have been implicated in binding to PI, promoting heterotetramerization of Get1/2 in the presence of Get3.<sup>38</sup> However, our crosslinking data suggest that WT Get2-1sc and Get2-1sc (K150A and K157A) similarly form heterotetramers in proteoliposomes even without Get3. Our proteoliposomes were prepared without PI, but still, we could detect heterotetramers of Get1/2 by channel recordings and chemical crosslinking. However, we cannot exclude the possibility that PI binding to Get1/2 survived during purification of Get2-1sc from *E. coli*. One possible explanation for PI binding to the pore-forming K150 and K157 residues is that it occludes the channel from leakage of small molecules through the Get1/2 channel. PI binding to the Get1/2 channel may be analogous to phospholipids entering into the Sec61 translocon channel that is partially opened by Sec63 in the absence of Sec62.<sup>48</sup> Another intriguing possibility is that PI binding could suppress Get1/2 channel activity to regulate insertion of TA proteins under certain physiological or pathological conditions. Further work is required to test these possibilities and determine the nature and role of PI binding to Get1/2.

### Get1/2 channel formation is required for TA protein release from Get3

Earlier biochemical and structural studies suggested a symmetric model where the long and flexible Get2 cytosolic domains bind on opposite sides of the Get3 dimer bound to a TA protein and bring it to the site of insertion.<sup>27,28</sup> When recruited, the cytosolic Get1 coiled-coil domains now bind on opposite sides of the Get3 dimer, inducing the Get3 open conformation and disrupting the TA binding site. Recent studies supported this model by solving the structure of the heterotetrameric Get1/2 complex.<sup>38</sup> Recent single-molecule fluorescence studies suggest that the heterodimer of the Get1/2 complex forms a minimal functional unit that mediates insertion of TA proteins by asymmetrically

binding to opposite sides of the Get3 homodimer.<sup>32</sup> However, it remains unclear how this asymmetric binding drives opening of the Get3 dimer to release TA substrates from Get3. Recent work suggests that the cytosolic domain of Get2 not only brings the targeting complex closer to the membrane but also initiates opening of Get3, which is then further opened by binding to the Get1 coiled coil.<sup>49</sup> Our studies are in line with the heterotetrameric Get1/2 model because the mutations of lysine residues in the heterotetramer interface disrupt the channel formation and thereby reduce TA protein insertion into the membrane. The substrate release assay reveals that the insertion defect of Get2-1sc (K150A and K157A) was caused by its inability to efficiently release TA substrates from Get3. This finding is consistent with the earlier observation that substrate release from Get3 is compromised by genetic disruptions of the Get1/2 TMDs.<sup>35</sup> We speculate that the channel-defective mutant inhibits movement of the cytosolic Get1 coiled-coil domains that are tightly linked to the membrane domains, whereas the channel dynamics would have little effect on long and flexible Get2 tethers. Thus, we suggest a model where opening and closing of the Get1/2 channel in the membrane accelerate movement of the cytosolic Get1 coiled-coil domain to bind and release TA substrate from Get3, allowing the substrate to directly land on the channel for insertion into the ER membrane (Figure 7). The calculated Get1/2 pore size of  $\sim 2.5$  nm would easily accommodate a typical  $\alpha$  helix TMD diameter of 1.0 nm<sup>50</sup> for insertion into the membrane.

Recent structural studies uncovered a membrane-embedded hydrophilic cavity on the cytosolic face of the Get1/2 structure.<sup>38</sup> Because this hydrophilic cavity resembles the cavity found in the YidC insertase,<sup>39</sup> it was proposed that the C-terminal hydrophilic tail of the TA protein is initially brought into the membrane via interactions with the hydrophilic cavity of the Get1/2 complex.<sup>38</sup> In light of our channel discovery, we propose that the hydrophilic cavity on the Get1/2 structure may provide a path for the TA TMD and its C-terminal segment to enter the channel, from which the TMD could laterally exit through the Get1/2 heterotetramer interface into the bilayer with concomitant translocation of their C-terminal tails into the lumen.

### Limitations of the study

There are multiple caveats associated with this study. (1) The presented results do not exclude the possibility that the Get1/2 heterodimer is sufficient for mediating TA protein insertion because our studies lack Get1/2 mutants that selectively disrupt formation of Get1/2 heterotetramers. (2) The TA protein release assay used in this study cannot discriminate whether the defect in TA protein release from Get3 is due to the defective Get1/2 channel or whether Get3 recaptures the released TA protein because of the defective channel's inability to efficiently insert TA proteins. Future work using a TA protein trap is needed to discriminate these two models. (3) Our conclusion of forming a heterotetrameric Get1/2 channel required for efficient TA protein release/insertion is derived from the engineered Get2/Get1sc construct. More studies using WT Get1/2 proteins are warranted to support this conclusion. Last, our data do not show whether the Get1/2 channel



also provides a path for the TMD of the TA substrate to access the lipid bilayer. Structure-guided mutagenesis studies combined with functional insertion assays are needed to test this possibility.

## STAR★METHODS

Detailed methods are provided in the online version of this paper and include the following:

- KEY RESOURCES TABLE
- RESOURCE AVAILABILITY
  - Lead contact
  - Materials availability
  - Data and code availability
- EXPERIMENTAL MODEL AND SUBJECT DETAILS
- METHOD DETAILS
  - DNA constructs
  - Purification of recombinant proteins
  - Reconstitution of Get1/2 proteins into small unilamellar vesicles (SUVs)
  - Analysis of Get1/2 orientation in SUVs
  - GFP and SRP encapsulation and leakage assay
  - Inner leaflet quenching assay
  - Protein-free liposome preparation
  - Formation of support-free suspended membrane containing Get1/2 proteins
  - Membrane conductance measurement
  - Preparation of radiolabeled VAMP2 and Get3 complex
  - Reconstitution of Get1/2 into proteoliposomes for TA protein insertion
  - TA protein insertion assay
  - Chemical crosslinking to monitor TA protein release from Get3
  - Membrane flotation assay
  - Predicted fraction of protein-free SUVs
  - Open section of a polygon made of  $\alpha$ -helices
- QUANTIFICATION AND STATISTICAL ANALYSIS

## SUPPLEMENTAL INFORMATION

Supplemental information can be found online at <https://doi.org/10.1016/j.celrep.2022.111921>.

## ACKNOWLEDGMENTS

We thank Robert Keenan for Get1, Get2, Get3, and Get2-1sc plasmids and Ramanujan Hegde for Get1, Get2, Get3, and 3F4 antibodies. M.M. was supported by NIH R01GM117386. P.H. was supported by Agence Nationale de la Recherche grant ANR-20-ERC9-0002.

## AUTHOR CONTRIBUTIONS

P.H., M.M., and F.P. designed the research. P.H. performed bulk fluorescence/microfluidic experiments and analyzed the data with F.P. J.A.C. purified and characterized recombinant Get2-1sc and its mutant. M.M. performed crosslinking, protease protection, and TA protein release experiments. J.M. prepared the targeting complex and performed the TA protein insertion assay with help from M.M. M.M., P.H., and F.P. wrote the manuscript with input from all authors.

## DECLARATION OF INTERESTS

The authors declare no competing interests.

## INCLUSION AND DIVERSITY

We support inclusive, diverse, and equitable conduct of research.

Received: May 31, 2021

Revised: November 7, 2022

Accepted: December 13, 2022

## REFERENCES

1. Eisenberg, D., Schwarz, E., Komaromy, M., and Wall, R. (1984). Analysis of membrane and surface protein sequences with the hydrophobic moment plot. *J. Mol. Biol.* 179, 125–142. [https://doi.org/10.1016/0022-2836\(84\)90309-7](https://doi.org/10.1016/0022-2836(84)90309-7).
2. Wallin, E., and von Heijne, G. (1998). Genome-wide analysis of integral membrane proteins from eubacterial, archaean, and eukaryotic organisms. *Protein Sci.* 7, 1029–1038. <https://doi.org/10.1002/pro.5560070420>.
3. Akopian, D., Shen, K., Zhang, X., and Shan, S.O. (2013). Signal recognition particle: an essential protein-targeting machine. *Annu. Rev. Biochem.* 82, 693–721. <https://doi.org/10.1146/annurev-biochem-072711-164732>.
4. Keenan, R.J., Freymann, D.M., Stroud, R.M., and Walter, P. (2001). The signal recognition particle. *Annu. Rev. Biochem.* 70, 755–775. <https://doi.org/10.1146/annurev.biochem.70.1.755>.
5. Guna, A., and Hegde, R.S. (2018). Transmembrane domain recognition during membrane protein biogenesis and quality control. *Curr. Biol.* 28, R498–R511. <https://doi.org/10.1016/j.cub.2018.02.004>.
6. Park, E., and Rapoport, T.A. (2012). Mechanisms of Sec61/SecY-mediated protein translocation across membranes. *Annu. Rev. Biophys.* 41, 21–40. <https://doi.org/10.1146/annurev-biophys-050511-102312>.
7. Li, L., Park, E., Ling, J., Ingram, J., Ploegh, H., and Rapoport, T.A. (2016). Crystal structure of a substrate-engaged SecY protein-translocation channel. *Nature* 537, 395–399. <https://doi.org/10.1038/nature17163>.
8. Voorhees, R.M., and Hegde, R.S. (2016). Structure of the Sec61 channel opened by a signal sequence. *Science* 351, 88–91. <https://doi.org/10.1126/science.aad4992>.
9. Voorhees, R.M., and Hegde, R.S. (2016). Toward a structural understanding of co-translational protein translocation. *Curr. Opin. Cell Biol.* 41, 91–99. <https://doi.org/10.1016/jceb.2016.04.009>.
10. Park, E., and Rapoport, T.A. (2011). Preserving the membrane barrier for small molecules during bacterial protein translocation. *Nature* 473, 239–242. <https://doi.org/10.1038/nature10014>.
11. Schuldiner, M., Metz, J., Schmid, V., Denic, V., Rakwalska, M., Schmitt, H.D., Schwappach, B., and Weissman, J.S. (2008). The GET complex mediates insertion of tail-anchored proteins into the ER membrane. *Cell* 134, 634–645. <https://doi.org/10.1016/j.cell.2008.06.025>.
12. Stefanovic, S., and Hegde, R.S. (2007). Identification of a targeting factor for posttranslational membrane protein insertion into the ER. *Cell* 128, 1147–1159. <https://doi.org/10.1016/j.cell.2007.01.036>.
13. Chartron, J.W., Clemons, W.M., Jr., and Suloway, C.J.M. (2012). The complex process of GETting tail-anchored membrane proteins to the ER. *Curr. Opin. Struct. Biol.* 22, 217–224. <https://doi.org/10.1016/j.sbi.2012.03.001>.
14. Chio, U.S., Cho, H., and Shan, S.O. (2017). Mechanisms of tail-anchored membrane protein targeting and insertion. *Annu. Rev. Cell Dev. Biol.* 33, 417–438. <https://doi.org/10.1146/annurev-cellbio-100616-060839>.
15. Denic, V., Dötsch, V., and Sinning, I. (2013). Endoplasmic reticulum targeting and insertion of tail-anchored membrane proteins by the GET pathway. *Cold Spring Harb. Perspect. Biol.* 5, a013334. <https://doi.org/10.1101/cshperspect.a013334>.



16. Hegde, R.S., and Keenan, R.J. (2011). Tail-anchored membrane protein insertion into the endoplasmic reticulum. *Nat. Rev. Mol. Cell Biol.* **12**, 787–798. <https://doi.org/10.1038/nrm3226>.
17. Johnson, N., Powis, K., and High, S. (2013). Post-translational translocation into the endoplasmic reticulum. *Biochim. Biophys. Acta* **1833**, 2403–2409. <https://doi.org/10.1016/j.bbamcr.2012.12.008>.
18. Favalaro, V., Spasic, M., Schwappach, B., and Dobberstein, B. (2008). Distinct targeting pathways for the membrane insertion of tail-anchored (TA) proteins. *J. Cell Sci.* **121**, 1832–1840. <https://doi.org/10.1242/jcs.020321>.
19. Kutay, U., Hartmann, E., and Rapoport, T.A. (1993). A class of membrane proteins with a C-terminal anchor. *Trends Cell Biol.* **3**, 72–75. [https://doi.org/10.1016/0962-8924\(93\)90066-a](https://doi.org/10.1016/0962-8924(93)90066-a).
20. Murphy, S.E., and Levine, T.P. (2016). VAP, a versatile access point for the endoplasmic reticulum: review and analysis of FFAT-like motifs in the VAPome. *Biochim. Biophys. Acta* **1861**, 952–961. <https://doi.org/10.1016/j.bbali.2016.02.009>.
21. Südhof, T.C., and Rothman, J.E. (2009). Membrane fusion: grappling with SNARE and SM proteins. *Science* **323**, 474–477. <https://doi.org/10.1126/science.1161748>.
22. Borgese, N., Colombo, S., and Pedrazzini, E. (2003). The tale of tail-anchored proteins: coming from the cytosol and looking for a membrane. *J. Cell Biol.* **161**, 1013–1019. <https://doi.org/10.1083/jcb.200303069>.
23. Kutay, U., Ahnert-Hilger, G., Hartmann, E., Wiedenmann, B., and Rapoport, T.A. (1995). Transport route for synaptobrevin via a novel pathway of insertion into the endoplasmic reticulum membrane. *EMBO J.* **14**, 217–223.
24. Mateja, A., Paduch, M., Chang, H.Y., Szydlowska, A., Kossiakoff, A.A., Hegde, R.S., and Keenan, R.J. (2015). Protein targeting. Structure of the Get3 targeting factor in complex with its membrane protein cargo. *Science* **347**, 1152–1155. <https://doi.org/10.1126/science.1261671>.
25. Rao, M., Okreglak, V., Chio, U.S., Cho, H., Walter, P., and Shan, S.O. (2016). Multiple selection filters ensure accurate tail-anchored membrane protein targeting. *Elife* **5**, e21301. <https://doi.org/10.7554/eLife.21301>.
26. Wang, F., Brown, E.C., Mak, G., Zhuang, J., and Denic, V. (2010). A chaperone cascade sorts proteins for posttranslational membrane insertion into the endoplasmic reticulum. *Mol. Cell* **40**, 159–171. <https://doi.org/10.1016/j.molcel.2010.08.038>.
27. Mariappan, M., Mateja, A., Dobosz, M., Bove, E., Hegde, R.S., and Keenan, R.J. (2011). The mechanism of membrane-associated steps in tail-anchored protein insertion. *Nature* **477**, 61–66. <https://doi.org/10.1038/nature10362>.
28. Stefer, S., Reitz, S., Wang, F., Wild, K., Pang, Y.Y., Schwarz, D., Bomke, J., Hein, C., Löhr, F., Bernhard, F., et al. (2011). Structural basis for tail-anchored membrane protein biogenesis by the Get3-receptor complex. *Science* **333**, 758–762. <https://doi.org/10.1126/science.1207125>.
29. Vilardi, F., Lorenz, H., and Dobberstein, B. (2011). WRB is the receptor for TRC40/Asn1-mediated insertion of tail-anchored proteins into the ER membrane. *J. Cell Sci.* **124**, 1301–1307. <https://doi.org/10.1242/jcs.084277>.
30. Wang, F., Whynot, A., Tung, M., and Denic, V. (2011). The mechanism of tail-anchored protein insertion into the ER membrane. *Mol. Cell* **43**, 738–750. <https://doi.org/10.1016/j.molcel.2011.07.020>.
31. Yamamoto, Y., and Sakisaka, T. (2012). Molecular machinery for insertion of tail-anchored membrane proteins into the endoplasmic reticulum membrane in mammalian cells. *Mol. Cell* **48**, 387–397. <https://doi.org/10.1016/j.molcel.2012.08.028>.
32. Zalisko, B.E., Chan, C., Denic, V., Rock, R.S., and Keenan, R.J. (2017). Tail-anchored protein insertion by a single Get1/2 heterodimer. *Cell Rep.* **20**, 2287–2293. <https://doi.org/10.1016/j.celrep.2017.08.035>.
33. Kubota, K., Yamagata, A., Sato, Y., Goto-Ito, S., and Fukai, S. (2012). Get1 stabilizes an open dimer conformation of get3 ATPase by binding two distinct interfaces. *J. Mol. Biol.* **422**, 366–375. <https://doi.org/10.1016/j.jmb.2012.05.045>.
34. Rome, M.E., Chio, U.S., Rao, M., Gristick, H., and Shan, S.O. (2014). Differential gradients of interaction affinities drive efficient targeting and recycling in the GET pathway. *Proc. Natl. Acad. Sci. USA* **111**, E4929–E4935. <https://doi.org/10.1073/pnas.1411284111>.
35. Wang, F., Chan, C., Weir, N.R., and Denic, V. (2014). The Get1/2 transmembrane complex is an endoplasmic-reticulum membrane protein insertase. *Nature* **512**, 441–444. <https://doi.org/10.1038/nature13471>.
36. Mateja, A., and Keenan, R.J. (2018). A structural perspective on tail-anchored protein biogenesis by the GET pathway. *Curr. Opin. Struct. Biol.* **51**, 195–202. <https://doi.org/10.1016/j.sbi.2018.07.009>.
37. Borgese, N., Coy-Vergara, J., Colombo, S.F., and Schwappach, B. (2019). The ways of tails: the GET pathway and more. *Protein J.* **38**, 289–305. <https://doi.org/10.1007/s10930-019-09845-4>.
38. McDowell, M.A., Heimes, M., Fiorentino, F., Mehmood, S., Farkas, Á., Coy-Vergara, J., Wu, D., Bolla, J.R., Schmid, V., Heinze, R., et al. (2020). Structural basis of tail-anchored membrane protein biogenesis by the GET insertase complex. *Mol. Cell* **80**, 72–86.e7. <https://doi.org/10.1016/j.molcel.2020.08.012>.
39. Kumazaki, K., Chiba, S., Takemoto, M., Furukawa, A., Nishiyama, K.i., Sugano, Y., Mori, T., Dohmae, N., Hirata, K., Nakada-Nakura, Y., et al. (2014). Structural basis of Sec-independent membrane protein insertion by YidC. *Nature* **509**, 516–520. <https://doi.org/10.1038/nature13167>.
40. Heo, P., Yang, Y., Han, K.Y., Kong, B., Shin, J.H., Jung, Y., Jeong, C., Shin, J., Shin, Y.K., Ha, T., and Kweon, D.H. (2016). A chemical controller of SNARE-driven membrane fusion that primes vesicles for Ca<sup>2+</sup>-triggered millisecond exocytosis. *J. Am. Chem. Soc.* **138**, 4512–4521. <https://doi.org/10.1021/jacs.5b13449>.
41. McIntyre, J.C., and Sleight, R.G. (1991). Fluorescence assay for phospholipid membrane asymmetry. *Biochemistry* **30**, 11819–11827. <https://doi.org/10.1021/bi00115a012>.
42. Ji, H., Coleman, J., Yang, R., Melia, T.J., Rothman, J.E., and Tareste, D. (2010). Protein determinants of SNARE-mediated lipid mixing. *Biophys. J.* **99**, 553–560. <https://doi.org/10.1016/j.bpj.2010.04.060>.
43. Heo, P., Ramakrishnan, S., Coleman, J., Rothman, J.E., Fleury, J.B., and Pincet, F. (2019). Highly reproducible physiological asymmetric membrane with freely diffusing embedded proteins in a 3D-printed microfluidic setup. *Small* **15**, e1900725. <https://doi.org/10.1002/smll.201900725>.
44. Song, L., Hobaugh, M.R., Shustak, C., Cheley, S., Bayley, H., and Gouaux, J.E. (1996). Structure of staphylococcal alpha-hemolysin, a heptameric transmembrane pore. *Science* **274**, 1859–1866. <https://doi.org/10.1126/science.274.5294.1859>.
45. Snapp, E. (2005). Design and use of fluorescent fusion proteins in cell biology. *Curr. Protoc. Cell Biol.* **27**, 21.4.1–21.4.13. <https://doi.org/10.1002/0471143030.cb2104s27>.
46. Auld, K.L., Hitchcock, A.L., Doherty, H.K., Fietze, S., Huang, L.S., and Silver, P.A. (2006). The conserved ATPase Get3/Arr4 modulates the activity of membrane-associated proteins in *Saccharomyces cerevisiae*. *Genetics* **174**, 215–227. <https://doi.org/10.1534/genetics.106.058362>.
47. Vilardi, F., Stephan, M., Clancy, A., Janshoff, A., and Schwappach, B. (2014). WRB and CAML are necessary and sufficient to mediate tail-anchored protein targeting to the ER membrane. *PLoS One* **9**, e85033. <https://doi.org/10.1371/journal.pone.0085033>.
48. Itskanov, S., Kuo, K.M., Gumbart, J.C., and Park, E. (2021). Stepwise gating of the Sec61 protein-conducting channel by Sec63 and Sec62. *Nat. Struct. Mol. Biol.* **28**, 162–172. <https://doi.org/10.1038/s41594-020-00541-x>.
49. Chio, U.S., Liu, Y., Chung, S., Shim, W.J., Chandrasekar, S., Weiss, S., and Shan, S.O. (2021). Subunit cooperation in the Get1/2 receptor promotes tail-anchored membrane protein insertion. *J. Cell Biol.* **220**, e202103079. <https://doi.org/10.1083/jcb.202103079>.

50. Bowie, J.U. (1997). Helix packing in membrane proteins. *J. Mol. Biol.* 272, 780–789. <https://doi.org/10.1006/jmbi.1997.1279>.
51. Mateja, A., Szlachcic, A., Downing, M.E., Dobosz, M., Mariappan, M., Hegde, R.S., and Keenan, R.J. (2009). The structural basis of tail-anchored membrane protein recognition by Get3. *Nature* 461, 361–366. <https://doi.org/10.1038/nature08319>.
52. Mariappan, M., Li, X., Stefanovic, S., Sharma, A., Mateja, A., Keenan, R.J., and Hegde, R.S. (2010). A ribosome-associating factor chaperones tail-anchored membrane proteins. *Nature* 466, 1120–1124. <https://doi.org/10.1038/nature09296>.
53. Studier, F.W. (2005). Protein production by auto-induction in high density shaking cultures. *Protein Expr. Purif.* 41, 207–234. <https://doi.org/10.1016/j.pep.2005.01.016>.
54. Heo, P., and Pincet, F. (2020). Freezing and piercing of in vitro asymmetric plasma membrane by alpha-synuclein. *Commun. Biol.* 3, 148. <https://doi.org/10.1038/s42003-020-0883-7>.
55. Tronchere, H., and Boal, F. (2017). Liposome flotation assays for phosphoinositide-protein interaction. *Bio. Protoc.* 7, e2169. <https://doi.org/10.21769/BioProtoc.2169>.

STAR★METHODS

KEY RESOURCES TABLE

REAGENT or RESOURCE	SOURCE	IDENTIFIER
<b>Antibodies</b>		
Rabbit anti-Get1	Mariappan et al. <sup>27</sup>	N/A
Rabbit anti-Get2	Mariappan et al. <sup>27</sup>	N/A
Rabbit anti-Get3	Mariappan et al. <sup>27</sup>	N/A
Rabbit anti-3F4	Stefanovic and Hegde <sup>12</sup>	N/A
<b>Bacterial and virus strains</b>		
<i>E. coli</i> Rosetta2/pLysS	Merck (Novagen)	Cat#71403
<i>E. coli</i> BL21 (DE3)	Merck (Novagen)	Cat#69450
<i>E. coli</i> LOBSTR-BL2 (DE3)	Kerafast	Cat#EC1002
<b>Chemicals, peptides, and recombinant proteins</b>		
SYLGARD™ 184 Silicone Elastomer Kit	Dow	Cat#1673921
1,2-dioleoyl-sn-glycero-3-phosphocholine	Avanti Polar Lipids	Cat#850375
1,2-dioleoyl-sn-glycero-3-phospho-L-serine	Avanti Polar Lipids	Cat#840035
Cholesterol	Avanti Polar Lipids	Cat#700000
1,2-dioleoyl-sn-glycero-3-phosphoethanolamine	Avanti Polar Lipids	Cat#850725
1,2-dioleoyl-sn-glycero-3-phospho-L-serine-N-(7-nitro-2-1,3-benzoxadiazol-4-yl)	Avanti Polar Lipids	Cat#810198
1,2-dioleoyl-sn-glycero-3-phosphoethanolamine-N-(lissamine rhodamine B sulfonyl)	Avanti Polar Lipids	Cat#810150
Sulforhodamine B	ThermoFisher	Cat#S1307
n-octyl-β-D-glucoside (OG)	Merck (Sigma-Aldrich)	Cat#08001
Deoxy Big CHAP	Calbiochem	Cat#86303-23-3
Lauryldimethylamine-N-Oxide	Anatrace	Cat#D360
n-Dodecyl-β-D-Maltopyranoside	Anatrace	Cat#D310
HEPES	Merck (Sigma-Aldrich)	Cat#H3375
KCl	Merck (Sigma-Aldrich)	Cat#60128
Slide-A-Lyzer™, 10 K MWCO	ThermoFisher	Cat#66380
SM2 Biobead	Bio-Rad	Cat#1523920
OptiPrep	Merck (Sigma-Aldrich)	Cat#D1556
Tris-HCl	Merck (Sigma-Aldrich)	Cat#T3253
Sodium dithionite	Merck (Sigma-Aldrich)	Cat#71699
ATP <sub>γ</sub> S	Merck (Sigma-Aldrich)	Cat#A1388
MgCl <sub>2</sub>	Merck (Sigma-Aldrich)	Cat#M8266
Squalene	ThermoFisher	Cat#10226790
Ni-NTA agarose	Qiagen	Cat#30230
BSA	Merck (Sigma-Aldrich)	Cat#A9418
Strep-Tactin Sepharose	IBA (Germany)	Cat#2-1201-010
Proteinase K	Roche	Cat#03115801001
α-Hemolysin	Sigma	Cat#H9395
<b>Oligonucleotides</b>		
Sec61β-26 tail-FW: CCCATGCTCAGATACACGAAT AAGACCAACATGAAACACATGGCC	This paper	N/A
Sec61β-26 tail-REV: ACAGCTGTAGTCTTCC TCTGAACCGGTGAAGTAAACTATGAT	This paper	N/A

(Continued on next page)

**Continued**

REAGENT or RESOURCE	SOURCE	IDENTIFIER
T7-2x Strep-Sec61 $\beta$ -FW: GAATACAAGCTG TAATACGACTCACTATAGGACCTGACACC ATGTCTGCCTGGAGCCACCCCAAGTTCCG AGAAGGGCGGCGGCAGCGGCGGCGGC AGCGGCGGCGGCAGCTGGAGCCACCC CCAGTTCGAGAAGGCCTCTCCTGGTCC GACCCCAAGTGGCACTAAC	This paper	N/A
SP64-REV: CAATACGCAAACCGCCTC	This paper	N/A
Get2 (KK/AA)-FW: ACCATTCTTGTGGCGT GGGTCTTTTTC	This paper	N/A
Get2 (KK/AA)-REV: AATGGTCCAGGCTGC CAGTCTGTTCAG	This paper	N/A
<b>Recombinant DNA</b>		
pET28 His-Get1	Mariappan et al. <sup>27</sup>	N/A
pET28 His-Get2	Mariappan et al. <sup>27</sup>	N/A
pET28 His-Get3	Mateja et al. <sup>51</sup>	N/A
pET28 Get2-Get1sc	Zalisko et al. <sup>32</sup>	N/A
pET28 Get2-Get1sc (K150A/K157A)	This study	N/A
SP64 Sec61 $\beta$ -VAMP2-3F4	Mariappan et al. <sup>52</sup>	N/A
SP64 Sec61 $\beta$ -VAMP2-3F4 plus 13 amino acids	This study	N/A
<b>Software and algorithms</b>		
Origin8	OriginLab	<a href="https://www.originlab.com/">https://www.originlab.com/</a>
ImageJ	ImageJ NIH	<a href="https://imagej.nih.gov/ij/download.html/">https://imagej.nih.gov/ij/download.html/</a>
Adobe Illustrator	Adobe	<a href="https://www.adobe.com/uk/creativecloud.html">https://www.adobe.com/uk/creativecloud.html</a>
FitMaster	Heka	<a href="https://www.heka.com/downloads/downloads_main.html#down_fitmaster">https://www.heka.com/downloads/downloads_main.html#down_fitmaster</a>
<b>Other</b>		
Titan2 (3D printer)	Kudo3D	N/A
EPC10 USB	HEKA Elektronik	Cat#895000
SpectraMax M5 Multi-Mode Microplate Reader	Molecular devices	M5

**RESOURCE AVAILABILITY**

**Lead contact**

Further information and requests for resources/reagents should be directed to and will be fulfilled by Malaiyalam Mariappan ([malaiyalam.mariappan@yale.edu](mailto:malaiyalam.mariappan@yale.edu)).

**Materials availability**

Image files and the mold for the microfluidic device fabrication are available from the [lead contact](#) with a completed Materials Transfer Agreement.

**Data and code availability**

- All data reported in this study will be shared by the [lead contact](#) upon request.
- This paper does not report original code.
- Any additional information required to reanalyze the data reported in this paper is available from the [lead contact](#) upon request.

## EXPERIMENTAL MODEL AND SUBJECT DETAILS

Proteins used for *in vitro* experiments were overexpressed and purified from *E. coli* of the BL21-DE3 (Merck), Rosetta2/pLysS (Merck), or LOBSTR-BL2 strain (Kerafast) listed in the [key resources table](#). Cells were cultured in Luria Broth (LB) or Terrific Broth (TB) at 37°C or 17°C, as described in [method details](#).

## METHOD DETAILS

### DNA constructs

cDNAs encoding full-length Get1, Get2, and Get3 were cloned into pET28 vectors carrying an N-terminal His-tag<sup>27,51</sup> using a standard cloning procedure. K150A and K157A mutations in Get2 were introduced into the Get2-1sc construct<sup>32</sup> using the Phusion site-directed mutagenesis protocol. The cDNA encoding human Sec61 $\beta$  cytosolic domain and the TMD of rat VAMP2 flanked by a 13 amino acid hydrophilic segment including the 3F4 epitope (TGTNMKHMAGAAA)<sup>52</sup> was cloned into the Sp64 vector. The Sp64 construct containing the coding region of Sec61 $\beta$ -VAMP2 TMD with a 26 amino acid hydrophilic segment (TGSEEDYSCPMLRYTNKTNMKHMAAA) was generated with the use of phosphorylated primers and Phusion DNA polymerase (NEB).

### Purification of recombinant proteins

His-Get1 and His-Get2 were individually transformed into *E. coli* Rosetta2/pLysS (Novagen). A single colony from LB/agar plates was inoculated into 10 mL Luria broth (LB) containing 50  $\mu$ g/mL kanamycin and 34  $\mu$ g/mL chloramphenicol and grown overnight. The preculture was used to inoculate 2 L of prewarmed homemade TB autoinduction medium<sup>53</sup> with an OD<sub>600</sub> of  $\sim$ 0.1, and the cells were grown for 18 h at 37°C and 200 rpm. The cells were then harvested by centrifugation using a JL10 rotor at 3000 g for 20 min at 4°C. Cell pellet was resuspended in 50 mL of Buffer A (50mM HEPES, pH 8.0, 500mM NaCl, 5% glycerol) supplemented with 10 mM imidazole and 1mM PMSF and homogenized using a PTFE/glass homogenizer with 10 passes. Cell suspension was subsequently lysed using a microfluidizer by passing through five times. After removal of cell debris by centrifugation (10,000  $\times$  g at 4°C for 20), the supernatant was centrifuged (Ti45 rotor at 40,000 rpm at 4°C for 1hr) to pellet the membranes, which were solubilized in Buffer A supplemented with 30mM imidazole and 0.5% n-dodecyl-N, N-dimethylamine-N-oxide (LDAO) for 1 h at 4°C. The membrane extract was cleared by centrifugation at 35,000 rpm for 40 min using a Ti45 rotor, and the supernatant was incubated with Ni-NTA beads at 4°C for 1hr. After collecting the flow-through, Ni-NTA beads were extensively washed with Buffer A supplemented with 0.1 LDAO and 30mM imidazole. Protein was eluted in buffer A containing 200 mM imidazole and 0.1% LDAO. The peak fractions analyzed by Coomassie staining were pooled and the concentration was determined by calculated A<sub>280</sub> extinction coefficients. Get1 and Get2 proteins are mixed at equal molar concentrations and the aliquots were flash-frozen in liquid nitrogen and stored at  $-80^{\circ}\text{C}$ .

pET28 His-Get3 was transformed into BL21 (DE3) cells and plated onto a kanamycin (50 $\mu$ g/mL) LB/agar plate. A fresh single colony was inoculated into a 100 mL LB supplemented with 30  $\mu$ g/mL Kanamycin and incubated overnight in a 37°C shaker. The overnight culture of OD<sub>600</sub> = 4.0 was added to 2L LB with 30  $\mu$ g/mL Kanamycin with a starting OD<sub>600</sub> of  $\sim$ 0.1 and incubated at 37°C and 250 rpm. When OD reached 0.9, the cells were induced with 0.1mM IPTG. Cells were harvested by centrifugation (JL10 rotor at 3000 g for 20 min at 4°C) after 3.5h of induction. Cell pellets were resuspended in Buffer T (50mM Tris-HCl pH 7.5, 500mM NaCl, 5% glycerol, 5mM BME, 10mM Imidazole) supplemented with 1mM PMSF and stirred for 15 min at 4°C. Cell suspension was lysed by passing 2x through a microfluidizer. Cell lysates were centrifuged at 15,000 rpm for 30 min using a JLA 17 rotor, and the supernatant was subjected to 5mL of Hi-Trap Ni-Sepharose column. The flow-through was collected and the column was sequentially washed with 50mL of Buffer T, and 50mL of Buffer T with 35mM imidazole. Get3 was eluted with Buffer T with 200mM imidazole. Peak Get3 fractions analyzed by Coomassie stain were pooled and dialyzed against 10mM Tris pH 7.5, 100mM NaCl, 40% glycerol, and 2mM DTT. Dialyzed Get3 was aliquoted, flash-frozen, and stored at  $-80^{\circ}\text{C}$ .

The single-chain Get2-1 or Get2-1 (KK/AA) was purified using the published protocol<sup>32</sup> with the following modifications. pET29b Get2-1sc or Get2-1sc carrying K150A and K157A mutations in Get2 was transformed into LOBSTR-BL2 (DE3)-RIL cells (Kerafast). A single colony was inoculated into 50mL of LB containing 50 mg/L kanamycin and 34 mg/L chloramphenicol and grown overnight at 37°C with shaking at 200 rpm. The TB for Get2-1sc expression was prepared by mixing 50 g/L Fisher LB and 0.5% (w/v) glycerol and sterilized by autoclaving. Before use, 1x potassium phosphate buffer was added to the TB from 10x stock (170 mM potassium phosphate and 720 mM dipotassium phosphate) along with antibiotics. 10 mL preculture OD600 of 1.5–2 was transferred to the prewarmed 2L TB and incubated at 37 °C at 200 rpm and grown until OD reached 0.6 to 0.7. The cultures were then moved to a 17°C incubator at 180 rpm. After 1hr, the cells were induced with 0.4 mM IPTG and grown for 17 h at 17 °C at 180 rpm. Cells were centrifuged with a JL10 rotor at 3000 g for 20 min at 4°C. Cell pellets from 2 L culture were resuspended in 50 mL Buffer B (50 mM HEPES, pH 8.0, 500 mM NaCl, and 10% glycerol) supplemented with 5 mM BME, 1 mM PMSF, 25  $\mu$ g/mL DNase, and 2 mM MgAc2 at 4°C. Cell pellets were scraped using a glass homogenizer rod and homogenized with 10 pumps in the 30 mL PTFE/glass homogenizer. Cells were lysed by passing through a microfluidizer with a pressure between 15 and 18K for 5 times. Cell lysates were spun at 10,000  $\times$  g at 4°C for 20 min to remove cell debris. Supernatants were spun again at 40,000 Ti45 rotor at 4°C for 2 h. Membrane pellets were resuspended with a paintbrush in 25 mL of DDM buffer (Buffer B supplemented with 25 mM imidazole, 5 mM BME, and 1% DDM).

Membrane suspension was further homogenized using a glass homogenizer with 5 passes. This suspension was ultracentrifuged for 1 h in a Ti45 rotor at 40,000 rpm at 4°C. Ni-NTA beads (2mL slurry for 2 L culture) were prewashed (2x rinse) with Buffer B (25 mM imidazole, 5 mM BME, and 0.3% DDM), and the washed beads were incubated with membrane extracts and gently rotated on a wheel at 4°C for 2h in a 50 mL falcon tube. Beads were washed for 3x with 40mL of Buffer B supplemented with 0.3% DDM buffer with 25 mM imidazole + 5mM BME. Beads were then transferred to a 10 mL column using 10mL of wash buffer. The column was washed twice again with 10 mL of the wash buffer with the following changes: (i) 300 mM NaCl and 25 mM imidazole; (ii) 150 mM NaCl and 50 mM imidazole. The Ni-NTA bound Get2-1sc was eluted with 8 successive 1 mL of Buffer B supplemented with 0.3% DDM, 5 mM BME, and 200 mM imidazole. Ni-NTA elutions were analyzed by 7.5% Tris-Tricine gels for Coomassie staining. Peak fractions of about 4 mL containing Get2-1sc were pooled and mixed with 1 mM EDTA and 0.1% n-Dodecyl-N, NDimethylamine-N-Oxide (LDAO). 15 mL Amicon filter with a 50 kDa cut-off was wet with 500  $\mu$ L Buffer B containing 0.3% DDM and 0.1% LDAO buffer and spun for 2 min at 3000 g. 4 mL of Ni-NTA elution were added to the filter and spun for 10min 4°C, and the spinning was repeated until 500  $\mu$ L remained. Concentrated samples were subjected to gel filtration using a Superdex 200 10/300 column equilibrated with 50 mM HEPES -KOH, pH 7.5, 200 mM NaCl, 5% glycerol, 0.1% LDAO, and 1 mM TCEP. Peak fractions were pooled and concentrated to  $\sim$ 2 mg/mL. Protein concentration was determined using a calculated extinction coefficient of Get2-1sc at  $A_{280}$ . 50 $\mu$ L aliquots were flash-frozen in liquid nitrogen and stored at  $-80^{\circ}\text{C}$ .

### Reconstitution of Get1/2 proteins into small unilamellar vesicles (SUVs)

Small unilamellar vesicles (SUVs) containing Get1/2 proteins were used for inner leaflet quenching assay and as carriers to form Get1/2 suspended membrane in the microfluidic device. All lipids, 1,2-dioleoyl-sn-glycero-3-phosphocholine (DOPC), 1,2-dioleoyl-sn-glycero-3-phospho-L-serine (DOPS), cholesterol (Chol), 1,2-dioleoyl-sn-glycero-3-phosphoethanolamine (DOPE), 1,2-dioleoyl-sn-glycero-3-phospho-L-serine-N-(7-nitro-2-1,3-benzoxadiazol-4-yl) (NBD-PS), were purchased from Avanti Polar lipids. Typically, 100 $\mu$ L of 3 mM of the lipid mixture (DOPC:DOPS:Chol:DOPE at 45:10:5:40 in mol%) was dried under nitrogen, rehydrated with the desired volume of HK buffer (25 mM HEPES, 150 mM KCl, pH7.4) supplemented with 1% n-octyl- $\beta$ -D-glucoside (OG) and Get1/2 at a 1:3500 protein: lipid ratio. For the inner leaflet quenching assay, 1.5 mol% of NBD-PS and 43.5 mol% of DOPC were used. After incubation for 30 min at 24°C, two times the initial volume of the HK buffer was added to the mixture to lower %OG below its critical micelle concentration. The remaining OG was removed by dialysis against 1 L HK buffer containing 0.1% w/v of SM2 Bio bead (Biorad) using a 10 kDa cut-off dialysis cassette (Thermo scientific).  $\sim$ 200 $\mu$ L of dialyzed proteoliposomes were retrieved from the cassette and mixed with  $\sim$ 200 $\mu$ L of 60% (OptiPrep, #D1556 from Sigma-Aldrich) in an ultracentrifuge tube. 150 $\mu$ L of 25% Optiprep was subsequently layered on the top of the 30%. Finally, 120 $\mu$ L of HK buffer was layered and centrifuged at 40000 rpm for 5 h SW41 Ti rotor at 4°C. The supernatant was collected and the presence of the incorporated Get1/2 proteins in SUVs was confirmed by running SDS-PAGE gel. The reconstitution process was the same for the other membrane proteins, tSNARE, vSNARE,  $\alpha$ -hemolysin, Get2-1sc, and Get2-1sc (K150A/K157A), except for the lipid-to-protein ratio as indicated in the figure legends.

### Analysis of Get1/2 orientation in SUVs

Get1/2, Get2-1sc, or Get2-1sc (K150A/K157A) SUVs were treated with or without 0.5 mg/mL proteinase K (PK) either in the presence or absence of 1% Triton X-100. Samples were incubated for 1h on ice followed by incubation with 5mM PMSF for 10min. PK was further inactivated by directly pipetting into boiling 2X SDS sample buffer and analyzed by immunoblotting with anti-Get1 antibodies raised against an epitope (AQDNYAKWTKNNRK) present in the cytosolic domain of Get1 or anti-Get2 antibodies raised against the Get2 N-terminal epitope (SELTEAEKRRL).<sup>27</sup>

### GFP and SRP encapsulation and leakage assay

For GFP encapsulation, the lipid film was prepared as above and dissolved in HK buffer containing 50  $\mu$ M GFP at a final lipid concentration of 20 mM. The mixture was frozen in liquid nitrogen and thawed in a water bath at 45°C for 1 min. After one more repeat of this cycle, the sample was extruded through a 100 nm polycarbonate filter (Avanti Polar Lipids). The Get1/2 complex was mixed with the GFP-liposome at the desired lipid to protein ratio by keeping  $\sim$ 1% OG. For SRB encapsulation, the lipid film was dissolved in HK buffer containing 1% OG, 10 mM SRB, and Get1/2 at the desired lipid to protein ratio at a final lipid concentration of 3mM. The detergent removal and liposome isolation steps for both GFP and SRB cases were carried out as described in the previous section. Aliquots of isolated SUVs in 100  $\mu$ M of lipid concentration were placed in a 96 well plate, and the GFP or SRB signal was measured for 10 min at 24°C.

### Inner leaflet quenching assay

The Reduction of NBD emission signal was measured using a spectrometer (plate-reader).<sup>40</sup> Aliquots of Get1/2-SUVs in 100  $\mu$ M of lipid concentration were placed in a 96 well plate, and the initial NBD signal was measured for 10 min at 24°C. 2 $\mu$ L of sodium dithionite stock solution (50 mM Tris-HCl, 2.5 mM sodium dithionite, pH 10.0) was added to the sample, and immediately NBD reduction signal was measured for 60 min at 24°C. Note that lowest NBD signal was negligible since 1–2% of the maximum NBD signal still remained even when SUVs were completely destroyed by a detergent. The sealing effect of Get3 was measured by adding Get3 (2.6  $\mu$ M or 26  $\mu$ M final concentration) to the well-containing Get1/2-SUVs for 20 min at 24°C. To test the effect of ATP, ATP- $\gamma$ S, MgCl<sub>2</sub> (both at 1 mM final concentration) and Get3 were added to Get1/2 SUVs before the NBD measurement.



### Protein-free liposome preparation

5 mM lipids of DOPC:DOPS:Chol:DOPE at 45:10:5:40 in mol% were dried under nitrogen and rehydrated with the desired volume of HK buffer. By keeping the mixture at 4°C, the tip of sonicator was directly immersed in the sample, and single pulse cycles of 5 s pulse and 5 s pause for 4 min were repeated three times with a pause of ≈2 min break between each pulse cycle. After formation, SUVs were kept at 4°C.

### Formation of support-free suspended membrane containing Get1/2 proteins

We prepared free-standing membrane containing Get1/2 using our recently developed method.<sup>43</sup> Briefly, the tip of syringe tube connected to the top microfluidic channel (resp. the bottom channel) contained 2 μL of the mixture composed of sonicated SUVs and the desired amount of Get1/2-SUVs (resp. 2 μL of sonicated SUVs only for the bottom channel) and the rest of the syringes was filled with HK buffer. The PDMS microfluidic device<sup>43</sup> was filled up with squalene and the two tubes were connected to the corresponding channel inlet. Then the device was carefully placed on the microscope stage of a confocal microscope (Eclipse Ti, Nikon) with add-ons of spinning disk (CSU-X, Yokogawa), image splitter (TuCam, Andor), and two cameras (iXon Ultra, Andor). To measure the electrical signals, two electrodes that are connected to the head-stage of the patch amplifier (EPC10 USB, HEKA) were inserted in the outlets of top and bottom channels. Each syringe injected the corresponding solution of 0.01 μL/s sequentially in the bottom and to channels. Consequently, ~1 nL of squalene droplet was trapped in the cylindrical hole where the support-free suspended membrane will be formed. Once the two electrodes were immersed in solution, the flow rate in each channel was reduced to 0.0012 μL/s. For an hour, two independent monolayers were formed at the two solution/squalene interfaces at the top and bottom of the squalene droplet by spontaneous fusion of SUVs. Upon Get1/2-SUVs spreading on top of the squalene droplet, it is expected that the hydrophilic cytosolic domains of Get1/2 remain in the aqueous HK buffer, while the hydrophobic TMDs inserts in the oil. Upon absorption of squalene by PDMS, the two leaflets contact and zip to form a bilayer. After bilayer zipping, hydrophilic cytosolic domains cannot cross the bilayer and will only be facing the channel in which the Get1/2-SUVs were flowed, indicating that, in theory, the orientation of Get1/2 can be controlled. The membrane formation was simultaneously monitored by capacitance measurement and microscopic observation of phase separation. Before the membrane formation, there were no remarkable signals in both optical and electrical observations. When the membrane was nucleated by a meeting of the two monolayers at the center of the hole, the capacitance started to increase. After the capacitance reached a plateau and the membrane was optically fully expanded, the Get1/2-membrane was stable for 3–4 h.

### Membrane conductance measurement

When the capacitance reached a plateau, a 100 mV voltage difference from top to bottom channel was applied, and the ionic current flow across the membrane was measured in 2 ms interval. Get1/2 channel formation was attested by stepwise conductance increase, as we measured previously for the pore formation by α-Synuclein.<sup>54</sup>

### Preparation of radiolabeled VAMP2 and Get3 complex

The PCR products encoding the 2x-Strep-tagged Sec61β-VAMP2 TMD<sup>27</sup> were synthesized by PCR using a 5' primer that encodes the 2x-Strep-tag, T7 promoter sequence, and start codon. This template was *in vitro* transcribed and translated in rabbit reticulocyte lysate supplemented with <sup>35</sup>S-methionine in the presence of 0.2 mg/mL His-Get3 (added from a 22 mg/mL stock in 10 mM Tris-HCl pH 7.5, 100 mM NaCl and 40% glycerol). A 1.5 mL translation reaction was diluted two-fold with ice-cold column buffer (20 mM HEPES-KOH, pH 7.4, 100 mM potassium acetate, 2 mM magnesium acetate, 1 mM DTT) and centrifuged for 30 min at 100,000 rpm in a TLA100.3 rotor at 4°C. The post-ribosomal supernatant was bound to a 300 μL DEAE-Sepharose fast flow column at 4°C, washed with 1 mL of column buffer, and eluted with a buffer containing 50 mM HEPES-KOH, pH 7.4, 350 mM potassium acetate, 7 mM magnesium acetate, and 1 mM DTT. The elution was passed over 250 μL Strep-Tactin agarose (IBA, Germany) three times. After washing one time with 0.3 mL of column buffer and 0.3 mL with Strep-Tactin buffer (SB: 50 mM HEPES-KOH, pH 7.4, 10% glycerol, 150 mM potassium acetate, 7 mM magnesium acetate, 1 mM DTT) at 4°C, the complex was eluted five times with 150 μL of SB containing 10 mM Desthiobiotin (Novagen). The peak fractions, measured by counting radioactivity, were pooled. The final sample contained ~7000 to 10,000 cpm/μL. The complex was either used immediately or frozen in aliquots in liquid nitrogen and stored at –80°C. The targeting complex containing Sec61β-VAMP2 TMD with a longer C-terminal segment (26 amino acids) was similarly prepared.

### Reconstitution of Get1/2 into proteoliposomes for TA protein insertion

Lipid solutions containing PC:PE: Rhodamine PE at a mass ratio of 8:1.9:0.1 were adjusted to 10 mM DTT and dried in a glass vial with a nitrogen flow for 15 min and incubated under vacuum for 2 h. Dried lipid films were rehydrated to a final concentration of 20 mg/mL in lipid buffer (50 mM HEPES-KOH, pH 7.4, 15% glycerol) and mixed for 2 h with intermittent vortexing. The lipid suspension was subjected to freeze-thaw cycles 10 times (freeze in liquid nitrogen; thaw at 50°C) and extruded at room temperature 21 times through 200-nm polycarbonate membranes using an Avanti mini-extruder. 100 μL single-use aliquots of the final clear liposome were flash-frozen in liquid nitrogen and stored at –80°C. For a standard reconstitution reaction, 100 μL of reconstitution buffer (RB: 50 mM HEPES-KOH, pH 7.4, 500 mM potassium acetate, 5 mM magnesium acetate, 250 mM sucrose, 1 mM DTT, 0.26% DBC) was mixed with 10 μL of liposome (200 μg) and purified Get2-1sc or Get2-1sc (KK/AA) at the desired concentration. Proteins

were excluded for the preparation of protein-free liposomes. This mixture was added to ~30 mg of Biobeads in a 0.5 mL tube and incubated for ~16 h at 4°C with end-over-end mixing. The fluid phase was recovered and mixed with a five-volume of ice-cold 20 mM HEPES pH 7.4 to dilute the residual detergent. The diluted liposomes were then sedimented in a TLA100.3 rotor in 1.5 mL micro-test tubes at 75,000 rpm for 30 min at 4°C. The proteoliposomes were resuspended in 25  $\mu$ L of membrane buffer containing 50 mM HEPES-KOH, pH 7.4, 100 mM potassium acetate, 5 mM magnesium acetate, 250 mM sucrose, and 1 mM DTT.

### TA protein insertion assay

Typically, 8  $\mu$ L of purified targeting complex was mixed with 1  $\mu$ L of 20 mM ATP and 1  $\mu$ L of either liposomes or reconstituted proteoliposomes. The reaction was incubated at 32°C for 30 min. After incubation, the samples were treated with proteinase K (0.5 mg/mL) for 60 min on ice, and the protease digestion terminated with 5 mM PMSF for 10 min on ice and further inactivated by transferring to 10-volumes of boiling 1% SDS/0.1M Tris pH 8.0 and boiled for 5 min. The samples were diluted with 1 mL of IP buffer (50 mM Tris-HCl pH 8.0, 150 mM NaCl, and 1% Triton X-100). The protease-protected fragments (PFs) were then immunoprecipitated using anti-3F4 antibodies directed against the C-terminus (KTNMKHMAAA) of TMDs of TA protein constructs. Immunoprecipitated products were analyzed by 12% Tris-Tricine SDS-PAGE and imaged by phosphorimaging. The bands were quantified by ImageJ (NIH).

### Chemical crosslinking to monitor TA protein release from Get3

The radiolabeled Get3-substrate complex was incubated with Get2-1sc or Get2-1sc (KK/AA) proteoliposomes as indicated in the figure legends for 30 min at 32°C. After incubation, the reactions were subjected to crosslinking with 0.2 mM disuccinimidyl suberate (DSS) for 30 min at room temperature. The reactions were quenched with 20 mM Tris-HCl pH 8.0 for 10 min. The samples were adjusted to 2x SDS sample buffer and analyzed by 10% SDS-PAGE/autoradiography after boiling. The remaining sample was diluted 10-fold in IP buffer and subjected to immunoprecipitation using anti-Get3 antibodies. The Get3-substrate crosslink was visualized by SDS-PAGE/autoradiography.

### Membrane flotation assay

The membrane flotation assay was modified from a previous protocol.<sup>55</sup> The radiolabeled Get3-substrate complex was incubated with protein-free liposomes, Get2-1sc proteoliposomes, or Get2-1sc (KK/AA) proteoliposomes for 10 min at room temperature. The reactions were then adjusted to 100  $\mu$ L with 1x salt buffer (HEPES-KOH, pH 7.4, 100 mM potassium acetate, 2 mM magnesium acetate) and mixed with an equal volume of 60% sucrose. 200  $\mu$ L of 30% sucrose containing vesicles and the targeting complex was layered on a 1 mL polycarbonate tube followed by 250  $\mu$ L of 25% sucrose and 50  $\mu$ L of 1x salt buffer. The samples were centrifuged for 1 h at 70,000 rpm on a TLA120.2 rotor with slower acceleration/deacceleration forces. 100  $\mu$ L (top), 200  $\mu$ L (middle), and 200  $\mu$ L (bottom) fractions were collected, TCA precipitated, and analyzed by autoradiography for VAMP2 and immunoblotting for Get2-1sc and Get3. The bands were quantified by ImageJ.

### Predicted fraction of protein-free SUVs

A heptamer of  $\alpha$ -hemolysin oriented in the same direction forms a channel through the membrane. Approximately 60% of H500 SUVs and 75% of H2000 SUVs do not have channels (see Figure 1B). Because proteins are likely lost/inactivated during the process, the actual lipid: active protein ratio in the SUV populations are expected to be lower than the input ones. Making the rough assumption that the proteins insert randomly without any cooperativity or interaction with a random orientation, it is possible to estimate these actual values since the fraction of SUVs without any channel can be expressed as:  $\sum_{n=1}^{\infty} P_n \cdot P_{pore}(n)$ , where  $P_n$  is the probability that an SUV contains  $n$   $\alpha$ -hemolysin molecules and  $P_{pore}(n)$  the probability that an SUV with  $n$   $\alpha$ -hemolysin can have at least one channel, i.e. 7  $\alpha$ -hemolysin oriented in the same direction.  $P_n$  follows a Poisson distribution:  $P_n = \frac{m^n e^{-m}}{n!}$ , where  $m$  is the average number of  $\alpha$ -hemolysin per SUV.  $P_{pore}(n) = 0$  for  $n < 7$ ,  $P_{pore}(n) = 2 \sum_{k=0}^{n-7} \binom{n}{k}$  for  $7 \leq n \leq 12$  and  $P_{pore}(n) = 1$  for  $n > 12$ . The results displayed in Figure S2 show that the final lipid:hemolysin ratio is ~2,300 for the H500 sample and ~3,000 for the H2000 sample, corresponding to a loss of 30%–80% of the proteins during the SUV preparation process, and proteins that are uninserted or simply stuck on the membrane surface.

It is possible to perform the reverse process and estimate the number  $i$  of Get1/2 complex per channel. Assuming up to 80% loss of Get1/2 during the SUV preparation process, the final lipid to Get1/2 ratio is between 3,500 and 20,000, i.e.  $m$  is between 1 and 6. The expression of  $P_{pore}(n)$  will depend on  $i$  and can be expressed as:  $P_{pore}(n) = 0$  for  $n < i$ ,  $P_{pore}(n) = 2 \sum_{k=0}^{n-i} \binom{n}{k}$  for  $i \leq n \leq 2i - 2$  and  $P_{pore}(n) = 1$  for  $n > 2i - 2$ . The corresponding curves for  $i = 1, 2$  and 3 are presented in Figure S2 and show that even though having 2 Get1/2 complex per channel is in the center of the acceptable range, a single or 3 Get1/2 complexes per channel is also possible.

### Open section of a polygon made of $\alpha$ -helices

Our assumption is that a channel is made by a fixed number of Get1/2 complexes that form a regular polygon. The open area of a channel made by  $\alpha$ -helices forming such regular polygon (yellow shaded region in Figure S4) can be estimated through basic geometry. Get1 and Get2 both contain 3 transmembrane domains, hence a single, two or three complexes will respectively

form a hexagon, a dodecagon and an octadecagon. The diameter of an  $\alpha$ -helix is in the range 1–1.3 nm. The open area of the cross-section of each polygon minus the area occupied by the  $\alpha$ -helices (yellow shaded area in [Figure S4](#)) can be calculated from simple geometry and is directly related to the diameter of the  $\alpha$ -helices,  $d$ :  $\frac{(3\sqrt{3} - \pi)d^2}{2}$  for the hexagon,  $\frac{(12(2 + \sqrt{3}) - 5\pi)d^2}{4}$  for the dodecagon,  $\frac{(36 \tan(\frac{4\pi}{9}) - 7\pi)d^2}{4}$  for the octadecagon. Varying  $d$  between 1 and 1.3 nm provides the range of predicted area for each case. These ranges can be compared to the measured area. Clearly the octadecagon is not acceptable because the area would be much too large compared to the actual. Hence the perimeter of the channel is made by less than three Get1/2 complexes. The area predicted by the dodecagon matches perfectly the measured area of the Get1/2 channel. The case of the hexagon is more complicated. The predicted area is smaller than the measured one (about half) but the prediction is based on a channel represented by a perfect cylinder with a regular hexagon cross-section. This is just an approximation. Hence, even though we favor a channel formed by two Get1/2 complexes, we cannot exclude that it is made by a single Get1/2 complex.

### QUANTIFICATION AND STATISTICAL ANALYSIS

Details regarding the statistical analysis of the data can be found within figure legends, as well as the [method details](#) section. Quantification of bands from immunoblots or autoradiographs was performed using ImageJ. Relative insertion in [Figures 6A](#) and [6B](#) was calculated by dividing the amount of the protease-protected fragment by the sample with the maximum protease-protected fragment. The percentage of TA protein release shown in [Figure 6D](#) was calculated from input autoradiograph by dividing the signal for Get3 x VAMP2 by the sum of the signals for Get3 x VAMP2 and uncrosslinked VAMP2. The percentage of PK-protected Get1 or Get2 fragments in [Figures S1C](#), [S1D](#) and [S5B](#), [S5C](#) was calculated by dividing the intensity of the PK-protected fragment by the total undigested band. The percentage shown underneath each fraction in [Figure S7](#) was calculated by dividing the sum of signals from the top, middle, and bottom fractions.